Hindawi Publishing Corporation
Journal of Sensors
Volume 2015, Article ID 805053, 18 pages
http://dx.doi.org/10.1155/2015/805053

Review Article

Optical Fiber Sensors Based on Nanoparticle-Embedded Coatings

Aitor Urrutia, Javier Goicoechea, and Francisco J. Arregui

Nanostructured Optical Devices Laboratory, Department of Electrical and Electronic Engineering, Public University of Navarre, Campus Arrosadía S/N, 31006 Pamplona, Spain

Correspondence should be addressed to Aitor Urrutia; aitor.urrutia@unavarra.es

Received 21 May 2015; Accepted 26 July 2015

Academic Editor: Wojtek J. Bock

The use of nanoparticles (NPs) in scientific applications has attracted the attention of many researchers in the last few years. The use of NPs can help researchers to tune the physical characteristics of the sensing coating (thickness, roughness, specific area, refractive index, etc.) leading to enhanced sensors with response time or sensitivity better than traditional sensing coatings. Additionally, NPs also offer other special properties that depend on their nanometric size, and this is also a source of new sensing applications. This review focuses on the current status of research in the use of NPs within coatings in optical fiber sensing. Most used sensing principles in fiber optics are briefly described and classified into several groups: absorbance-based sensors, interferometric sensors, fluorescence-based sensors, fiber grating sensors, and resonance-based sensors, among others. For each sensor group, specific examples of the utilization of NP-embedded coatings in their sensing structure are reported.

1. Introduction

For the last few decades optical fiber sensors have experimented an important growth and relevance in sensing technologies field. Recently, many applications have been developed to monitor or detect a wide range of parameters in different fields such as biomedicine, aeronautics, environmental control, and other industries. This interest of the scientific community in optical fiber sensors is motivated by their already well-known advantages, as immunity to electromagnetic interferences, remote sensing, small dimensions, low weight, biocompatibility, real time monitoring, or multiplexing capabilities [1, 2].

Currently, optical fiber sensors field has increased in its research lines and possibilities with the use of nanocoating deposition techniques. Nanostructured thin films and nanocoatings have been applied to the diverse optical fiber configurations for the fabrication of new sensors. Thanks to these combinations, many devices have been developed obtaining the detection and monitoring of multiple parameters such as a wide range of gases [3, 4], pH [5], temperature [6], humidity [7, 8], ions [9], and biomolecules [10, 11].

One of the latest steps in the search for improved novel sensors is the inclusion of nanoparticles (NPs) within coatings. In diverse new researches, it has been demonstrated that selected NP-embedded coatings enhance some parameters of previous devices, for example, sensitivity [12, 13], dynamic range, robustness, and lifetime. On one hand, these improvements are due to the fact that NPs can provide additional special properties in coatings (mesoporosity, higher roughness, antibacterial behavior, etc.). Thus, higher surface area in sensitive regions allows reaching lower limits of detection (LoD) in biosensing. On the other hand, the intrinsic properties of certain NPs cause diverse phenomena by their own, for example, localized surface plasmon resonances (LSPR) or quantum confinement.

In the following sections, most used sensing principles and optical fiber configurations will be described, and then their combination with diverse NP-embedded coatings will also be presented. The optical fiber sensors described in this paper are classified into several groups depending on their detection method. Intensity-based sensors, interferometric sensors, fluorescence-based sensors, fiber grating sensors, and resonance-based sensors are the most typical ones.

2. Intensity- and Absorbance-Based Sensors

2.1. Introduction. Intensity-based optical fiber sensors have been reported since the 70s in literature, and their development has been widely used to these days. Generally, the underlying phenomenon of such sensors is the light transmission-absorption in materials. Absorbance is based on the attenuation of light due to the characteristics of the material that light is guided through. The sensitive materials change the absorbance in presence of a specific parameter or analyte, and therefore a change on the guided light can be observed. The absorption mechanisms are described by the Lambert-Beer Law, where the transmission of the light through an analyte, material, or sensitive region (T, called transmittance) represents the relation between the light intensity before (I_o) and that after (I) passing through this sensitive region, expressed by the following equation:

$$T = \frac{I}{I_o} = 10^{-\alpha L} = 10^{\varepsilon CL}, \quad (1)$$

where L is the length of interaction within the absorbing region (optical path) and α is the absorption coefficient which can be denoted as the product of the molar absorptivity (ε) and the concentration (C) of the target. This transmittance nomenclature can also be transferred to absorbance terms, such that

$$A = -\log_{10}\frac{I}{I_o} = \alpha L = \varepsilon CL, \quad (2)$$

where absorbance (A) is the magnitude commonly used in this kind of optical fiber sensors.

The incorporation of sensitive materials to optical fiber sensors can be performed by embedding them into coatings or thin films. The propagation of light through the optical fiber presents two contributions: the guided field in the core and the evanescent field in the medium surrounding this core. This evanescent field is not accessible in unmodified standard cladded fibers, and therefore it is not relevant to sensing. Thereby, the external medium cannot interact with the guided light through the core, nor the evanescent contribution in the cladding. Nevertheless, when the cladding is intentionally replaced by sensitive coatings, there could be a significant interaction between the external medium and the evanescent field to the guided light. The optical properties of the selected coating materials determine the changes in this evanescent-field interaction. In many cases, optical configurations are developed to enlarge this interaction with the evanescent field by removing the cladding, bending, or tapering the fiber, as it is shown in Figure 1, thus improving their sensitivity to the changes in the external media.

2.2. Cladding-Removed Optical Fiber Sensors. Cladding-removed optical fiber (CROF) is one of the simplest structures used in optical fiber sensing (shown in Figure 1(a)). A short distance of the cladding of the fiber is removed and then replaced by the deposition of a selected nanostructured coating which interacts with the surroundings. This coating acts as sensitive region, and therefore its composition and fabrication parameters are thoroughly studied in order to improve sensitivity or other desirable sensing values. Thin film fabrication techniques such as Layer-by-Layer (LbL) assembly, Langmuir-Blodgett, sol-gel, or spin-coating are used to create these coatings, where in some cases NPs are embedded inside them.

During the last two decades many CROF based approaches have been developed. Nevertheless, as it was previously commented, the use of NPs in coatings has not been reported until the last few years.

CROF sensors with NP-based coatings have been reported in several works, detecting humidity [14, 15], ethanol [16], ammonia [17], methanol [18], and other gases [19, 20]. For instance, Kodaira et al. [20] coated an optical fiber with SiO_2 NPs and poly(diallyldimethyl ammonium chloride) to create mesoporous overlays by LbL. The resultant coating morphology allows allocating functional chemical compounds for diverse gases detection. Another relevant approach is reported by Mariammal et al. [16], using SnO_2 and $CuO{:}SnO_2$ NPs for ethanol detection. The use of $CuO{:}SnO_2$ NPs based coatings presented an enhancement of 3 times in sensitivity with respect to previously reported sensors based on pure SnO_2 NPs.

2.3. Bent Optical Fiber Sensors. Bent optical fiber sensors can be considered as a particular case of the CROF sensors, when the modified fragment of the fiber is submitted to a significant bending (see Figure 1(b)). Sometimes these devices are also reported as U-shape fiber sensors [21]. The intentionally bending effect provides higher losses in the transmitted light and dramatically increases the evanescent-field depth [8, 22]. Khijwania et al. demonstrated the notable enhancement in sensitivity presented by a U-probe in comparison with a straight probe due to a larger evanescent field and absorption coefficient [8]. Included in this classification, there are different devices which have sensitive coatings without NPs for humidity [8, 23, 24] or pH [25]. However the use of coatings with NPs has appeared more recently. Thus, Guo and Tao reported ammonia sensing devices [26] based on Ag NPs within silica coatings with a theoretical limit of detection (LoD) of 61 ppb. Vijayan et al. developed optical fiber humidity sensors based on a Co NPs-embedded polyaniline coating [27]. Their sensors showed a quick response of 8 s in a broad dynamic range of 20–95% in relative humidity terms. Another humidity device with MgO NPs was presented by Shukla et al. [28] using the sol-gel technique. Also U-bent fibers have been coated with Au NPs to develop resonance-based sensors [29, 30], as it will be described in Section 6.

2.4. Tapered Optical Fiber Sensors and Other Special Fiber Sensors. An alternative strategy for exposing the evanescent field to an external sensitive coating is fiber tapering. This technique modifies the optical fiber geometry and its structure (see Figure 1(c)) thus obtaining an increment of the interaction of light with the sensitive region and therefore providing higher variations in the magnitude of the evanescent field. The length and waist diameter of the taper, the refractive indices, and other fiber parameters were analyzed by Ahmad and Hench using a ray model. The influence of these factors on the penetration depth of the evanescent

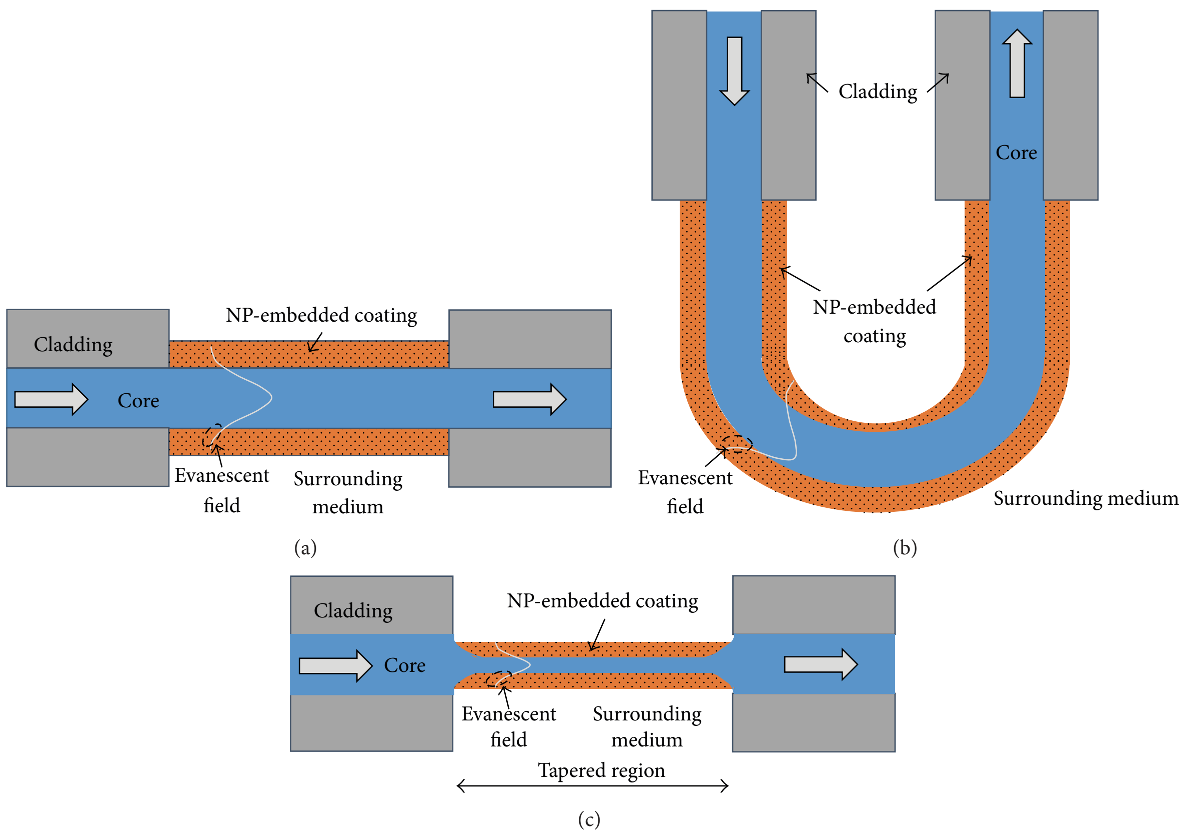

Figure 1: Schematic of the most used optical configurations used for the development of absorbance-based sensors with NP-embedded coatings: (a) cladding-removed fiber; (b) U-shape or bent fiber; (c) tapered fiber. Evanescent field is also depicted as tails that penetrate and interact within the coating.

field was studied [31]. They concluded that the longest tapers provided the largest evanescent field and that penetration depth can be augmented three times with a convenient waist diameter depending on the original fiber diameter, according to other studies [32, 33].

Recently, tapered optical fiber sensors with Ag NPs-based coatings have been developed for ammonia sensing [34], ethanol levels [35], and bacteria detection [36]. Another example of this type of devices was presented by Monzón-Hernández et al. for hydrogen sensing using PaAu NPs [37].

The combination of diverse special fibers with NPs-embedded coatings is also reported. Examples of this are such as hollow core fibers with Fe_3O_4 NPs for magnetic field sensing and optical filter purposes [38], polished fibers with TiO_2 NPs [39], or photonic crystal fibers (PCFs) in junction with Au NPs [40] and Fe_3O_4 NPs [41] for temperature sensing. D-fibers also have been coated with silica NPs coatings to develop other sensing approaches [42]. PCFs and microstructured optical fibers (MOFs) are recently used in the development of new sensors with metallic NPs based on metal-enhanced fluorescence (MEF) or surface-enhanced Raman scattering (SERS) (reported in Sections 4 and 5, resp.).

3. Interferometric-Based Sensors

3.1. Introduction. Optical fiber interferometers have been widely used in the development of optical fiber sensors. They can be mainly classified into four types: Fabry-Perot, Mach-Zehnder, Michelson, and Sagnac [43]. Their sensing principles and then some examples of each type of sensors with NP-embedded coatings will be described below.

3.2. Fabry-Perot Interferometers. The fabrication of Fabry-Perot interferometers (FPI) in optical fibers has provided different sensing structures. There are numerous works that use the simplest FP configuration: an air gap between two perpendicularly cleaved optical fibers [44, 45]. A modification of this basic structure involves the fabrication of a polymer-based nanocavity onto the cleaved end-face of the optical fiber. These FPI nanocavities based on nanostructured coatings have been commonly performed by means of the LbL technique in the last decade [46, 47]. Thus, the obtained optical system is composed of three different materials in terms of refractive index: the optical fiber (n_f), the nanocavity (n_c), and the surrounding medium (n_e). When the transmitted light passes through the structure, the two media interfaces (fiber-coating and coating-air) act as partial mirrors, where part of the optical power is transmitted and the other part is reflected (see Figure 2). The reflected power depends on the RI of the three materials and the nanocoating thickness (cavity length).

This reflective phenomenon has been used for sensing applications. Some of them have performed Fabry-Perot cavities including NPs within thin films. For instance, silica

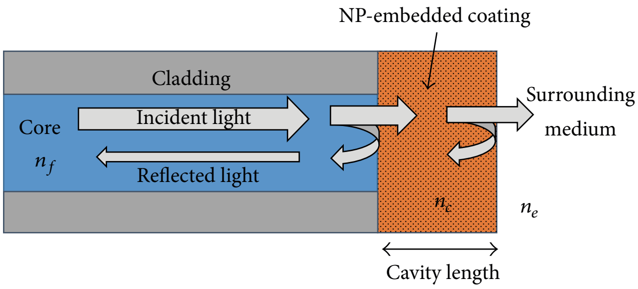

FIGURE 2: Schematic of the Fabry-Perot interferometer configuration in optical fiber sensing.

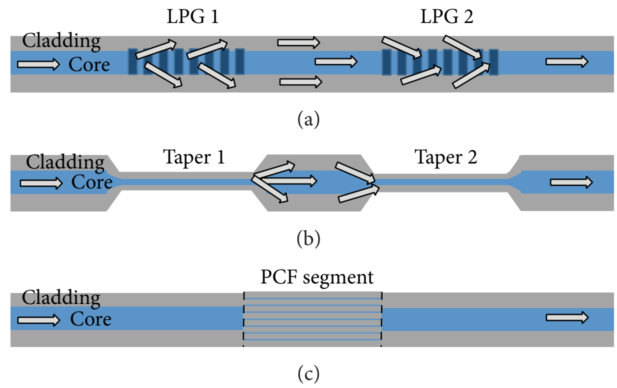

FIGURE 3: Schematic of the mainly used MZ configurations in optical fiber sensing: (a) based on Long-Period Gratings (LPGs); (b) based on tapered fibers; and (c) based on a PCF.

NPs were used in FPI based sensors for humidity [48, 49]. Moreover, FPI based sensors with embedded Au NPs or TiO_2 NPs have been published for biological applications such as rabbit immunoglobulin detection [50] or even as a precision refractometry for refractive index (RI) monitoring [51]. Another example is the addition of carbon nanotubes based nanocomposites in Langmuir-Blodgett overlays to detect volatile organic compounds (VOCs), reported by Consales et al. [52]. Furthermore, Yin et al. presented a novel pH sensor whose nanocavity was composed of polymeric overlays combined with complex NPs [53]. In another report, Ag NPs were allocated in zeolite thin films to detect Hg^{2+} cations in aqueous solutions [54].

3.3. Mach-Zehnder Interferometers. The multiple configurations provided by the Mach-Zehnder (MZ) interferometers had led to a wide variety of sensing applications. At their beginning, these types of interferometers were composed of two separate light paths or arms: the sensing path and the reference path. The light entered into the device and was split into two beams by a fiber coupler. Then, light passed through both paths reaching to another fiber coupler, where lightbeams were reunited and both contributions create the interference. The traditional MZ structure was scaled down as it was applied to optical fiber devices. In Figure 3, different approaches to MZ configurations are shown.

Since the introduction of fiber gratings in sensing, many sensors have been performed including them in the MZ configuration [55, 56], shown in Figure 3(a). As it will be detailed in Section 6, the periodic perturbation of the grating produces the coupling of some core modes to cladding-propagating modes, thus obtaining two virtual paths for the transmitted light in a single optical fiber. To recombine both light contributions, a second grating is placed behind the first one, obtaining the desirable interference. The sensing mechanism of the fiber grating is described in *Fiber Grating Sensors*. One experimental work based on this configuration is presented by James et al. [57], coating two Long-Period Gratings with embedded SiO_2 NPs in polymeric thin films by LbL. In this study, the response of the system to the environmental perturbations was investigated, to measure the changes for temperature and RI and also to detect ammonia concentrations.

Regarding the rest of MZ configurations, there are some relevant works for diverse applications. For instance, Li et al. [58] presented one MZ based sensor using ultra-abrupt tapered fibers to detect N_2, with an improved RI sensitivity with respect to a conventional MZ interferometer. In another approach, Socorro et al. have reported a theoretical and experimental study of the multimode interferences created by a single mode-multimode-single mode fiber structure, obtaining a sensitivity enhancement controlling the thickness of thin films [59]. However until these days, as in the FPI situation, the use of NPs in the MZ based approaches is not very common.

3.4. Michelson Interferometers. Another interesting type of interferometers is that called Michelson interferometers (MI). Their optical structure is quite similar to the MZ devices, but in this case, the light is reflected at the end of each arm by a mirror addition. Also this approach can be developed in a compacted configuration, commonly known as in-line Michelson interferometers. As in the case of MZ interferometers, LPGs have been mainly used in MI configurations. There are recent advances in MZ with NP-embedded coatings for concretes applications. One of the most relevant works is reported by Carrasquilla et al., who design a LPG based MI interferometer [60]. LPGs were coated with Au NPs entrapped in a sol-gel matrix to create a platform for the immobilization of functional structure-switching DNA aptamer molecules.

3.5. Sagnac Interferometers. Sagnac interferometers present an interesting alternative to other sensing structures, due to advantages as easy fabrication and simple set-up and robustness. These types of interferometers consist of an optical fiber loop, along which two beams are propagating in counter directions with different polarization states, providing the desired interference. A more detailed description of those interferometers can be found in the bibliography [61]. Mainly, Sagnac interferometers are commonly fabricated using high birefringent fibers or polarization maintaining (PM) fibers to obtain a higher sensitivity, although, more recently, they have been developed using PCFs or PM-PCFs, reducing their temperature dependency.

Sagnac interferometers designed with NP-embedded coatings have not been reported. However there are some advances where the sensing fiber has been coated with polymers. Hence, humidity sensors based in chitosan [62] or polyvinyl(alcohol) [63] or salinity sensing devices based in polyimide [64] have been published.

4. Fluorescence-Based Sensors

4.1. Introduction. The use of fluorescence as a sensing mechanism for optical fiber sensors has been studied for decades because of two main reasons. On one hand fluorescence has been a daily life tool for scientific disciplines such as microbiology, and therefore researchers have an abundant repertoire of different fluorescent labels and dyes and a good knowledge of how to bond them to other target molecules. On the other hand the optical nature of the fluorescent signal is ideal to be collected and transmitted through a medium such as an optical fiber. The wide variety of fluorescent dyes together with the benefits of the optical fiber as transmission medium (low losses, wide broadband, multiplexing, small size, biocompatibility, etc.) has encouraged the research in this field for decades.

Although there are a lot of works in the bibliography that reports fluorescent based optical fiber sensors [65–69], not all of them describe optical sensing approaches in which nanoparticles are present. Most of the traditional approaches for fluorescent optical fiber sensors describe the use of regular fluorescent organic molecules that experience a variation in their emission efficiency due to the presence of the analyte. Strictly speaking most of them are intensity-based sensors, although it is possible to find other approaches such as phase-fluorescence sensors [70, 71]. Nevertheless there have been two fields where nanoparticles have brought a significant improvement of the fluorescent properties of the materials and it is possible to use it in the field of sensors, the use of semiconductor quantum dots and the fluorescence enhancement in the surroundings of certain metallic particles. The main contributions and trends are summarized in the next subsections.

4.2. Quantum-Dot Based Sensors. As it was commented in the previous introduction, one of the main advantages of fluorescence-based sensors is that after decades of research in fields such as microbiology there is an enormous available diversity of available fluorophores [72, 73] and there are also well-known tools for manipulating those molecules, including selectively binding to other molecules and structures. Nevertheless, traditional organic fluorophores have some important drawbacks; usually they show short lifetimes and very restricted excitation wavelength ranges too close from the fluorescence emission maximum (small Stokes shifts typically around 10–20 nm). These two limitations are very important when a sensor is being designed and implemented because they negatively impact in the sensitivity and in the lifetime of the sensors. Quantum dots overcome those critical limitations of the organic fluorophores.

Fluorescent quantum dots (QDs) are nanoparticles of semiconductor material with a diameter of typically around 3–8 nm. Such nanosize of the semiconductor particle induces the phenomenon of the quantum confinement. The excited electron-hole pair behaves as a quasiparticle called exciton and this quasiparticle has some physical dimensions related to its Böhr radius that depend on the specific properties of the semiconductor material. When the exciton size is constrained by potential barriers, the density of energy state distribution (DOS) is significantly altered, changing from a continuous DOS distribution of the bulk materials to a discrete DOS typical of the QDs [74]. One of the most important advantages of QDs is that their absorption spectrum is very broad and remains almost unaltered as the size of the QD decreases, and at the same time the narrow fluorescence emission peak shows a significant blue-shift as the quantum confinement is increased (with smaller QDs). This absorbance and emission characteristic is very useful since it overcomes the problem of the small Stokes shift of the traditional organic fluorophores and allows adjusting the excitation wavelength and intensity so it is possible to avoid spectral overlapping between the excitation and the emission.

Depending on the size of the QD nanoparticles the fluorescence emission can be tuned from the near infrared to the blue region of the visible spectrum. Although there are different approaches for achieving quantum confinement and consequently the QDs, the wet-synthesis routes of semiconductor nanoparticles are the most used ones. Such wet chemistry approaches are reproducible and cost-effective, and currently there are several synthesis routes available using organic solvents or even water-based approaches. Typically QDs are chalcogenide semiconductors, most of them from group VI: CdTe, CdSe, ZnSe, ZnS, and so forth. One of the most important advantages of nanoparticle QDs is that they can be easily functionalized using well developed surface chemistry, and they can be embedded or bonded to a wide variety of surfaces and matrices [75].

There are a lot of sensing applications based on QDs luminescence. Their high quantum yield has made possible applications such as single particle tracking using fluorescence microscopy [76], very useful for intracellular dynamics research. Functionalized QDs have been used successfully in selective cell identification techniques, both *in vitro* [77] and *in vivo* [78]. Other sensing applications have been reported based on colloidal dispersions of QDs that selectively graft to biological molecules such as proteins [79, 80] or even sensing mechanisms based on the variation of the fluorescent signal using biologically triggered Förster Resonance Energy Transfer (FRET) quenching [81, 82]. Optical fiber sensors have also been reported using quantum dots. Their high quantum yield and small size make them suitable for embedding into sensitive thin films over the optical fibers. It is possible to find coatings for transmission tapered fibers and d-shaped or similar approaches using a tapered end fiber in a reflection arrangement [83]. The versatility of QDs allowed being incorporated into thin films created inside the inner holes of PCFs to create a fluorescent temperature optical sensor [84] (Figure 4).

4.3. Fluorescence Enhancement Using Metallic Nanoparticles. There is another phenomenon that involves fluorescence

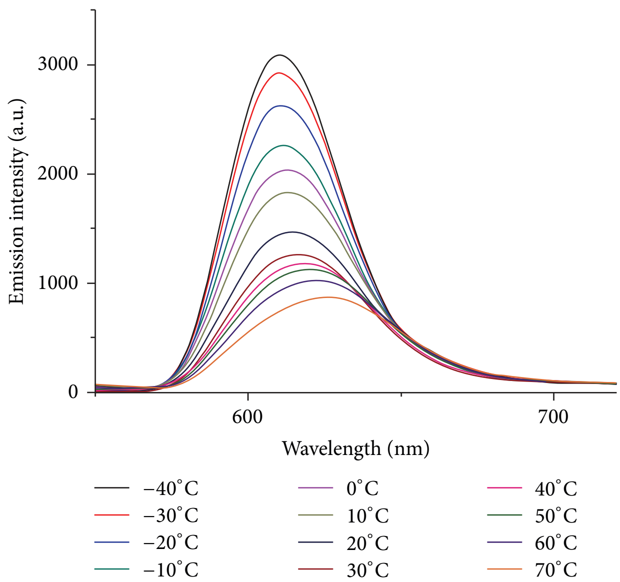

Figure 4: Temperature sensor using CdSe QDs embedded into LbL thin films fabricated inside the inner holes of a PCF. Reprinted with permission from [84].

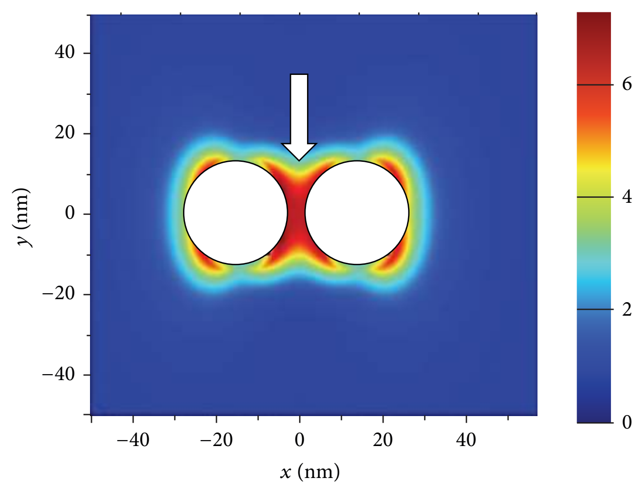

Figure 5: Electric field intensity in the vicinity of two Ag NPs of 25 nm diameter separated 30 nm between centers. Simulated using Greensym. It is possible to see that the region between both particles (pointed to with an arrow) shows a significant increasing in the electrical field intensity.

that is a direct consequence of the nanostructure of certain particles. This phenomenon is known as metal-enhanced fluorescence (MEF), and it is caused by the alteration of the normal radiative and nonradiative decay rates caused by the close proximity of metal nanoparticles. The MEF phenomenon is caused by the singular concentration of the local electrical field in the surroundings of certain metallic nanoparticles as a consequence of a resonant phenomenon known as localized surface plasmon resonance (LSPR). LSPR is the collective oscillation of the free electrons of metallic nanoparticles due to their resonant coupling with incident light at a specific wavelength. More detailed information about the nature and applications of the LSPR phenomenon can be found in the bibliography [85]. The LSPR absorption peaks of metallic nanoparticles have been widely used in the development of optical fiber sensors [15, 86].

The electrical field in the medium surrounding the metallic nanoparticles is altered, and as it is shown in Figure 5 when two nanoparticles come very close one to the other, a dramatic enhancement of the local electrical field is caused in the nanoparticles gap. If a fluorophore molecule is placed in this region its emission properties of fluorophores are significantly enhanced by both the excitation and emission modifications.

It has been probed that the distance of the fluorophores to the nanoparticles surface is a critical parameter to achieve MEF. The fluorophore is needed to be close enough to the plasmonic nanostructure, since the field enhancement decays nearly exponentially with distance from the metallic surface. Nevertheless if the fluorophore is too close to the NP (less than 5 nm) its fluorescence would be quenched significantly due to the nonradiative decay through energy and/or charge transfer to the metal. Consequently the distance of the fluorophores should be controlled in a range of 5 to 30 nm in general.

Liu's group had reported a DNA-detecting platform based on MEF, using Ag NPs, PDDA/PSS LbL films, and conjugated polyelectrolytes [87, 88]. But the polyelectrolytes can also play a significant role in the development of optical sensors as far as the MEF could be manipulated in an *in situ* way by external stimuli such as pH or temperature variations. Based on this concept, pH sensitive poly(acrylic acid)/PDDA spacer layers over Ag NPs that change their thickness with their ionization degree have been reported, and consequently the MEF is altered [89].

It has also been demonstrated that sharp shapes and edges of metallic nanoparticles induce more intense electromagnetic field concentrations and consequently higher MEF rates. Consequently nonspherical nanoparticles are frequently used in the development of optical sensors based on MEF. For example, gold nanorods have been successfully used to create glucose sensors [90] among other applications. Gabudean et al. even have demonstrated that gold nanorods can be used as dual probes for MEF and for surface-enhanced Raman spectroscopy (SERS) [91] (Figure 6). SERS sensing mechanism and applications will be commented in the following paragraphs.

5. Surface-Enhanced Raman Spectroscopy (SERS)

Sensors are devices designed for the quantitative identification of analytes but there are other applications in which the qualitative characterization of the analyte is crucial, such as in molecule identification. In such applications there are several analytic techniques available (High Pressure Liquid Chromatography (HPLC) and other chromatography techniques) that helps to determine the composition of the chemicals

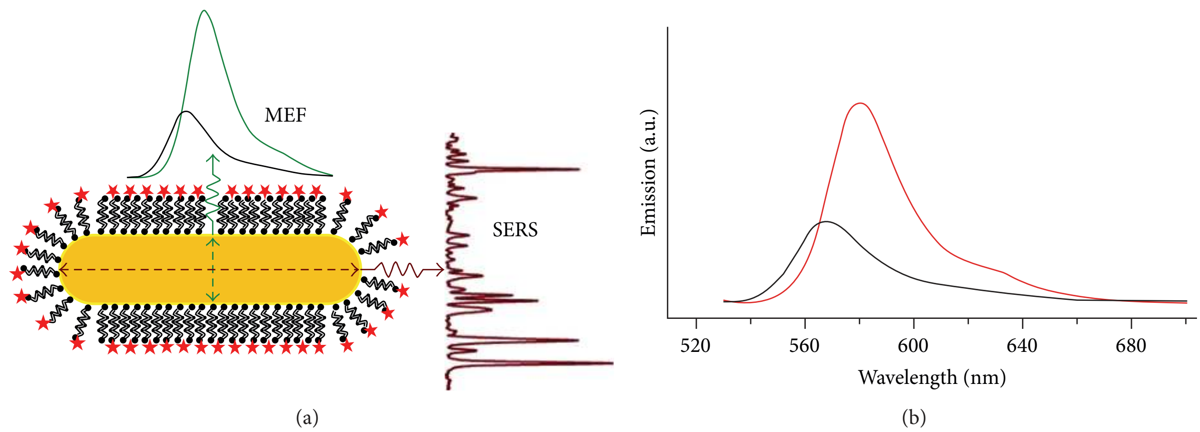

Figure 6: (a) Schematic configuration of a gold nanorod dual MEF and SERS probe. (b) Fluorescence spectra showing a 2-fold enhancement of the Rose Bengal emission. Reprinted with permission from [91]. © (2012) American Chemical Society.

present in the sample. Nevertheless there are techniques that provide information about the structure, chemical bonds, or presence of certain functional groups and moieties as far as they are based on the excitation of the natural vibrational frequencies of the molecules. The most used ones are Fourier Transform Infrared (FTIR) and Raman spectroscopy. In fact Raman spectroscopy is especially useful because it makes it possible to distinguish between very similar structures but generally it requires powerful lasers and long acquisition times to get a weak Raman scattering signal.

As it is has been previously commented the electrical field concentrations in the vicinity of metallic nanoparticles by means of LSPR coupling allow the apparition of two different enhancement phenomena, MEF and SERS. Therefore when the LSPR induced electromagnetic field concentration occurs near metallic nanoparticles, the molecules nearby the surface experiment an enhancement in their Raman scattering cross section, making more efficient their excitation. Enhancements up to 8 orders of magnitude in the Raman scattering emission are typically observed from the molecules surrounding the metallic nanoparticles [92].

The very first approaches used highly rough metallic substrates obtained by several oxidation-reduction cycles of the surface of the metal, but the electrical field concentration spots were randomly distributed throughout the surface and this made difficult the utilization of SERS as a tool for quantitative determination of chemical species.

More sophisticated structures such as the so-called Nanosphere Lithography (NSL) technique or the Metal Film Over Nanosphere (MFON) have been successfully used to fabricate the metallic structures that allow the electromagnetic field concentrations that make the SERS phenomenon possible (Figure 7). Both techniques have been widely used but both of them have been used over planar substrates and not over optical fibers where the geometry is much more complicated.

Although most of the applications are focused on planar substrates for Lab-On-a-Chip (LOC) applications [95, 96], optical fiber approaches have been also reported using nanoparticle decorated tapered optical fibers [94, 97–100]. Another example can be found in [94] where it is reported that silver nanoplates were deposited on the tapered surface of an optical fiber with the LbL technology (Figure 8).

6. Fiber Grating Sensors

6.1. Introduction. Fiber gratings are optical fibers that present a periodic perturbation of their optical properties, namely, the core refractive index. Since the 80s decade fiber gratings have contributed to the development of many devices for diverse applications in research fields such as communications, instrumentation, and sensing. There are several techniques for fabricating optical fiber gratings based on UV laser [101], CO_2 [102], infrared [103] lasers, or electric arc [104]. It is possible to find two main kinds of optical fiber gratings, Fiber Bragg Gratings (FBGs) and Long-Period Gratings (LPGs). LPGs are characterized by the long periodicity of their perturbation, which ranges from 100 um to 1000 um. In the FBGs case, the perturbation has a shorter period than LPGs (tens of microns). This difference in period results in different optical phenomena that yield different spectral behavior when white light is guided through the grating. In LPGs, certain nonpropagating core modes are visible in the transmission spectrum at wavelengths where there is a coupling between the core and the copropagating cladding modes, whereas, in FBGs, there is a coupling between propagating and counterpropagating core modes. Each attenuation band presented in the spectrum is a consequence of an optical resonance of the guided light and the grating structure, so it is frequent to refer to those transmission minima as resonance wavelengths.

On one hand, for FBGs, the resonance wavelength obeys the Bragg condition described as [105]

$$\lambda_{\text{bragg}} = 2n_{\text{eff,core}}\Lambda_g. \quad (3)$$

More details about FBGs can be found in relevant works reported by Hill and Meltz [105], Kersey et al. [106], or Erdogan [107].

On the other hand, for LPGs the resonance condition is given by [108]

$$\lambda_{\text{res}} = \left(n_{\text{eff,core}} - n_{\text{eff,clad}}\right)\Lambda_g, \quad (4)$$

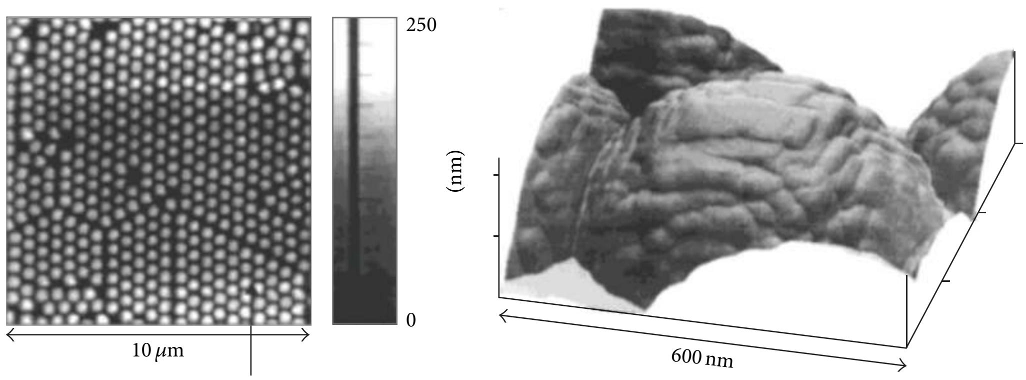

(a) (b)

Figure 7: (a) AFM image of a silver coated assembly of polystyrene nanospheres of 540 nm diameter. A continuous metallic film was created over the nanospheres. (b) 3D reconstruction of the AFM micrography where the sharp edges in the metallic film can be observed. It is in those regions where SERS takes place. Reprinted with permission from [93]. © (2002) American Chemical Society.

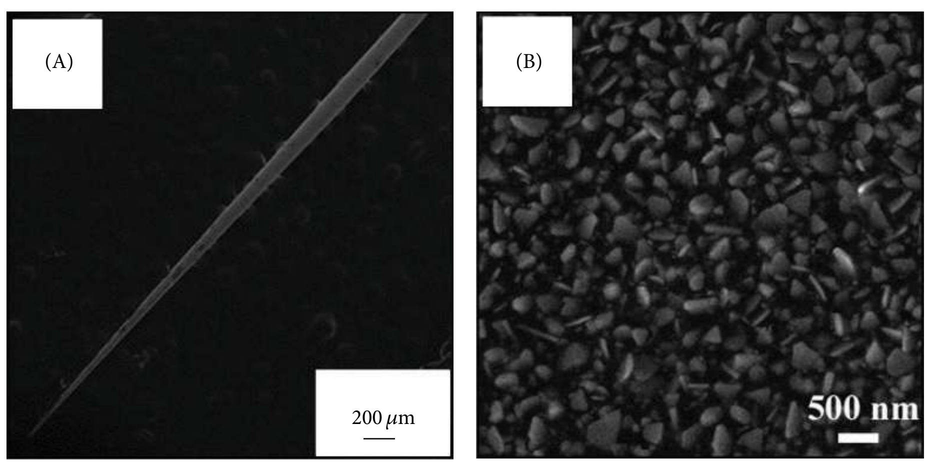

(a)

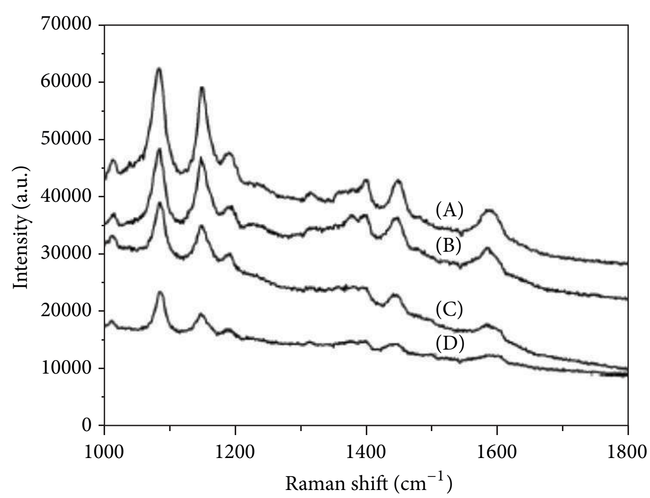

(b)

Figure 8: (a): (A) low- and (B) high-magnification SEM images of a SERS probe made from a tapered optical fiber. It is possible to see the rough profile of the silver nanoparticles synthesized onto the surface of the taper. (b): SERS spectra of 4-ATP (10^{-7} M) detected by the tapered fiber probes with different cone angles; (A) 3.5, (B) 9.6, (C) 15.8, and (D) 22.6. Reproduced with permission from [94]. © (2014) AIP Publishing LLC.

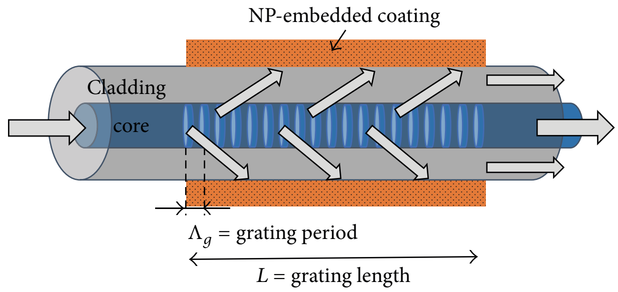

Figure 9: Illustration of a LPG coated with a NP-embedded coating.

where λ_{res} is the resonance wavelengths, $n_{eff,core}$ and $n_{eff,clad}$ are the effective refractive indices of the core and the cladding, respectively, and Λ_g represents the grating period along the fiber axis (see Figure 9). LPG theory and some of its optical sensing applications are found in the bibliography [109, 110].

Both FBGs and LPGs have been widely used for the fabrication of optical fiber sensor devices and sensor networks. The following sections describe and enumerate briefly several research works based on FBGs and LPGs. Also, several recent applications with the use of NPs within coatings as sensitive regions onto these fibers are presented.

6.2. FBG and Tilted FBG Sensors with NP-Embedded Coatings. FBG sensors have been widely reported in literature during the last 25 years for the monitoring of numerous physical parameters, including vibration [111], strain [112], bending, temperature [113], and pressure [114].

An important particular type of FBGs is the tilted FBGs (TFBGs), where their grating has a shift in angle with respect to the fiber axis [115]. TFBGs based sensors have been also developed to measure strain and temperature [116, 117], vibration [118], bending [119], torsion [120], external refractive index [121], or humidity [122] among other parameters.

All FBG sensors reported in the two previous paragraphs do not present NPs in their coatings, or even in some cases they do not have any coating as sensitive region. Works with coated FBGs as sensor have also been reported recently with gold nanofilms [123] for biosensing and with ZnO thin films [124] for an enhancement in RI sensitivity. Thus, Paladino et al. [125] studied the effect of the thickness of the coating and the RI in TFBG sensors. As in other fiber optics structure sensors, the use of NPs into optical fiber sensing applications is very recent and it was during the last few years when most of the applications were reported. In the particular FBG sensors case, there are few works which add NPs or nanocomposites. For example, Lepinay et al. introduced gold NPs to create novel biosensors based on TFBGs [12]. The Au NPs were coated onto the TFBG, thus providing an enhanced sensing platform for protein detection. Another work which presents a novel refractometer with an improvement in sensitivity is reported by Bialiayeu et al. [126], where a TFBG was coated with silver nanowires, obtaining a 3.5-fold increase in sensitivity with respect to the uncoated TFBG.

6.3. LPG and Coated LPGs Sensors without NPs. As in FBGs, the inherent LPG structure also permits the development of sensors for temperature, bending, strain, or external RI depending on their fabrication settings [63]. The sensitivity to a particular measurand is dependent upon the period of the LPG and the order of the cladding mode to which the guided optical power is coupled and thus is different for each attenuation band. These characteristics make them attractive for sensing purposes.

Cusano et al. studied theoretically and experimentally the effects of the cladding modes along the LPG structure when this was coated with nanoscale overlays [127]. The variations of the external RI and the thickness of the coating were analyzed, showing relevant improvements in the surrounding RI in terms of amplitude variation and wavelength shift in the attenuation bands [83, 84]. As a result of these investigations several optochemical sensors based on polystyrene nanocoatings have been reported by the same research group [128–130]. Langmuir-Blodgett [131], LbL [132], and sputtering [133] deposition techniques were used for the fabrication of diverse thin film coatings over the LPGs for sensing various physical and chemical magnitudes such as hydrogen [134, 135], pH [136], humidity [137], VOCs [138], or the study of sensitive improvements [139, 140]. Another relevant study was reported by Shu et al. [141], presenting the so-called turning points in LPGs. These turning points appeared for LPGs with specific grating periods and provide two resonance wavelengths for each cladding mode, thus allowing the fabrication of high sensitivity devices [142].

6.4. LPG Sensors with NPs-Embedded Coatings. During the last few years, the inclusion of NPs in coated LPGs has been also reported for different sensing applications. In Table 1, some of these works are presented, including target, type of nanoparticles included, coating composition, and fabrication method used. A wide variety of substances have been monitored such as ethanol, ammonia, proteins, or other low-molecular analytes. One of the most used deposition techniques for LPG sensitive coating fabrication is LbL, because this method allows a controllable management of the thickness and the NP composition of the fabricated thin films.

An interesting work about how to improve the sensitivity in humidity LPG sensors is reported by Viegas et al. [13]. They demonstrated that the use of SiO_2 nanospheres in polymeric thin films as intermediate structural coatings enhanced the humidity sensitivity by a factor of 1.5 at a RH ≈ 30%, which was improved to a value of 3.5 when dealing with RH around 70% (shown in Figure 10).

7. Resonance-Based Optical Fiber Sensors

7.1. Introduction. Resonance-based sensors are another important group within optical fiber sensing field. Their development has been reported for more than 20 years. When an optical waveguide is coated by a nanostructured coating, the transmission of light along the overall structure can be affected. Depending on the properties of the different materials involved in the system (the waveguide, the coating, and

Table 1: Summary of optical fiber sensors with NP-embedded coatings based on LPGs. Specific terms of sensitivity parameters, relative humidity (RH), limit of detection (LoD), parts per billion (ppb), refractive index units (RIU), and enhancement with respect to the same device without NPs (ENH).

Target	Nanoparticles	Deposition technique	Sensitivity parameters	Reference
Humidity	SiO_2 NPs	LbL	0.2 nm/RH%	[143]
Ion chloride	Au colloids	LbL	0.46 nm/RH%	[13, 144]
Ethanol	ZnO nanorods	Aqueous chemical growth	LoD ≈ 0.04%	[145]
Ammonia	SiO_2 NPs	LbL	—	[146]
Low-molecular chemicals	TiO_2 NPs	LbL	LoD = 140 ppb	[147, 148]
RI	SiO_2 NPs	LbL	10^{-7} M	[149]
Proteins	SiO_2 and Au NPs	LbL	1927 nm/RIU	[150]
Aromatic carboxylic acids	SiO_2 NPs	LbL	19 nM	[151]
Low-molecular analytes	Au NPs	Sol-gel	1 nM	[152]
Corrosion	Fe and SiO_2 NPs	Dip-coating	~2- and ~2.5-fold ENH for ATP and QDNA	[60]
Sucrose, RI	Au NPs	LbL	—	[153, 154]
Copper	Cibacron blue	LbL	20 nm ENH/RIU	[155]

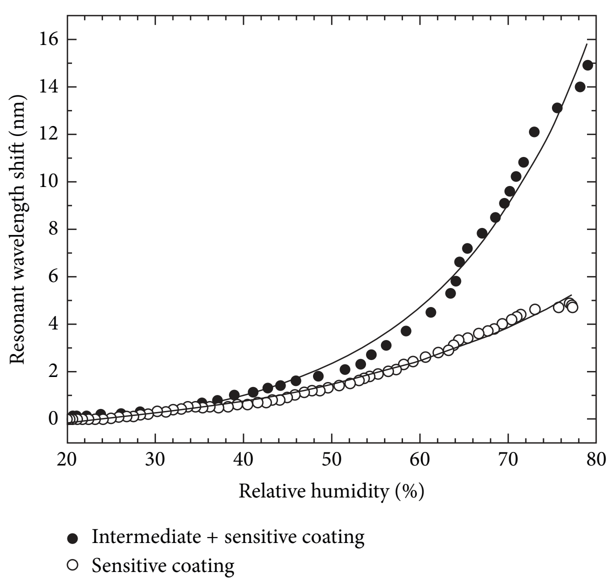

Figure 10: Resonance wavelength shift dependence with the humidity for LPG with (black spots) and without (white spots) SiO_2 NPs intermediate coatings [13], from the journal "*SENSORS*."

the surrounding medium), three different kinds of electromagnetic resonances can be recognized. To distinguish these types of resonances, the relationship of the permittivity of the coating (ε_2), composed of real and imaginary part, is considered (see Figure 11).

The first resonant phenomenon happens when the real part of ε_2 satisfies the following three conditions: it must be negative; it must be higher in magnitude than its respective imaginary part; and it must be higher in magnitude than both the waveguide permittivity and the surrounding permittivity as well. Under these conditions, the produced resonance is called SPR. This kind of resonance consists in the coupling of the energy of certain resonant wavelengths of the incident light to a surface electrical current in a metallic-semiconductor interface. When such resonance occurs the energy is transferred from photons to electrons, and therefore such wavelengths are not observable in the final transmitted light.

The second type of resonance occurs when the real part of ε_2 satisfies these other three conditions: it must be positive; it must be higher in magnitude than its respective imaginary part; and it must be higher in magnitude than both the waveguide permittivity and surrounding permittivity as well; see Figure 11. Some studies demonstrated that the propagation of light in semiconductor cladded waveguides exhibits some attenuation maxima for specific thickness values of the semiconductor cladding and, also, at certain wavelengths of incidence values [170]. This is due to a coupling between waveguide modes and a specific lossy mode of the semiconductor thin film [171]. Because of that, in these cases, resonances are denoted as lossy mode resonances (LMRs) [156, 172]. In this resonance the light couples into a different propagating medium, and it is lost from the transmitted light.

Finally, a third case happens when the real part of ε_2 is close to zero, and its imaginary part is large. This particular case, named as long-range surface exciton polariton (LRSEP), has not been applied to the development of optical fiber sensors and will not be reported in this review.

According to the optical structure, resonance-based sensors could be englobed as a subgroup of absorbance sensors, grating sensors, or interferometric sensors if their coatings satisfy the concrete resonance conditions. Generally in literature, resonance-based sensors are considered as a group by themselves because of the importance of the resonance phenomena. However, they could also be classified as CROF sensors, U-shape sensors, tapered sensors, LPG sensors, FBG sensors, and so forth, depending on their optical configuration.

As the SPR and LMR based sensors with NP-embedded coatings have being widely reported in the last few years, they will be described in separate sections.

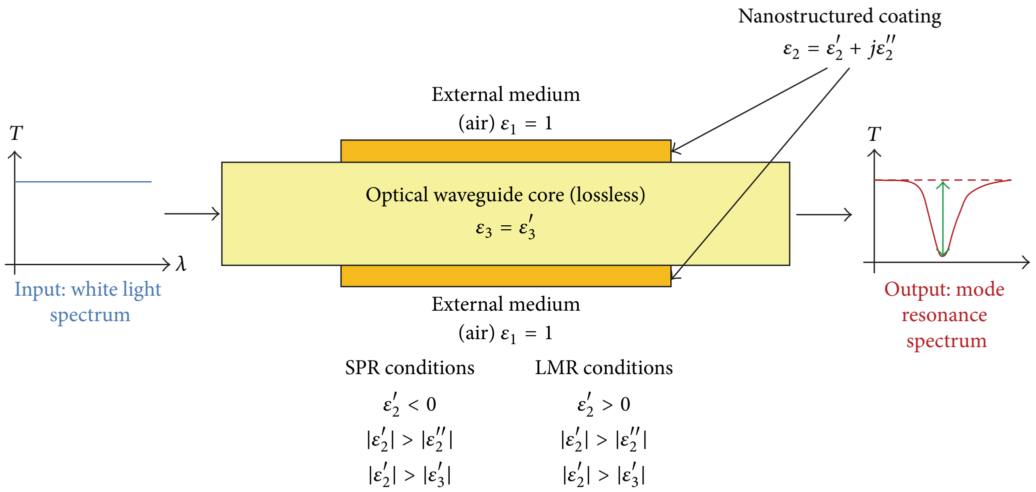

FIGURE 11: Schematic of a waveguide coated with a nanostructured film and the required conditions to generate SPR and/or LMR. Adapted from [156]. Copyright (2014) with permission from Elsevier.

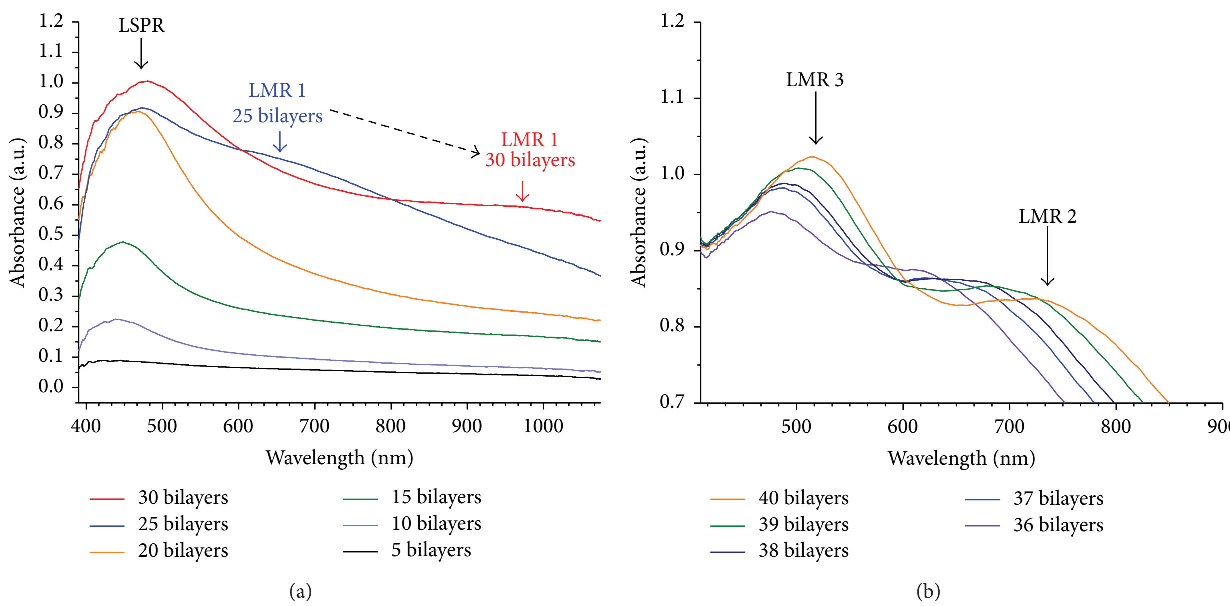

FIGURE 12: UV-Vis absorption of the sensor in function of the number of LbL bilayers: (a) 1–30 bilayers; (b) 35–40 bilayers. Reprinted from [157], Copyright (2012) with permission from Elsevier.

7.2. SPR and LSPR Based Sensors. Since the introduction of optical fiber technology in the research of the technique of SPR, fiber-optic SPR sensors have presented a lot of advancements. Jorgenson and Yee published in 1993 [173] one of the earliest optical fiber sensors based on SPR. They studied the changes of the transmission spectrum varying the key parameters: the film thickness, the film refractive index, and the length of the coated area. After that, many devices based on SPR phenomenon were reported thanks to the metallic thin coatings onto the fiber, being an essential reference in biochemical sensing in the last decade [174]. However, these metallic coatings mainly composed of silver or gold films do not contain NPs, and consequently there are not SPR based sensors with NP-embedded coatings.

The unique optical properties of metal NPs have also attracted the sensor community to develop LSPR based sensors [175]. In the LSPR phenomenon, the conductive NPs interact with the light which goes through the coatings, generating resonance waves. This occurs when the dimension of the NPs is smaller than the wavelength of light. The created localized resonances depend on the size, geometry, and composition of NPs and their distribution in the coatings. LSPR based sensors have few advantages over SPR based sensors, such as higher surface area, and it is now when they are becoming relevant [176] as they are improving sensitivity ratios or limit of detection values [12] or selectivity. Nevertheless, further studies will be required. Hence, Cao et al. [177] performed a comparative study between a LSPR

Table 2: Summary of optical fiber sensors based on LSPR and LMR phenomena.

Resonance phenomenon	Target	Coating	Deposition technique	Sensitivity parameters	Reference
LSPR	HF	Au NPs and silica matrix	Sol-gel	1% to 5%	[158]
LSPR	Hydrogen peroxide	Ag NPs embedded in polyvinyl(alcohol)	Dipping and sintering	10^{-8} M	[159]
LSPR	Proteins	APTMS, glutaraldehyde/cysteamine + Au NPs (nanocages or nanospheres)	LbL	11 pM (nanospheres) 8 pM (nanocages)	[12]
LSPR	Anti-IgG	Amino silane + Au NPs	Silanization	0.8 nM	[160]
LSPR	Proteins	Poly(ethyleneimine)/Au NPs + poly(sodium 4-styrenesulfonate)	LbL	—	[161]
LSPR	Blood glucose	Au NPs + glucose oxidase	LbL	Blood min. volume ~ 150 μL	[162]
LSPR	Explosive vapours	Au NPs functionalized with 4-mercaptobenzoic acid, l-cysteine, and cysteamine	Silanization with APTES	<100 nM (23 ppb) LoD ~ 5–10 ppb	[30]
LSPR	DNA sequences	Au NPs functionalized with oligonucleotides	LbL	<100 nM	[163]
LSPR & LMR	Humidity	Poly(allylamine hydrochloride)/poly(acrylic acid) + Ag NPs	LbL	~1 nm/RH%	[157]
LSPR & LMR	RI	Poly(allylamine hydrochloride)/poly(acrylic acid) + Au NPs	LbL	4037 nm/RIU LMR 2 1906 nm/RIU LMR 3	[164]
LMR	RI	TiO_2 NPs/poly(sodium 4-styrenesulfonate)	LbL	2872.73 nm/RIU 1987 nm/RIU	[165, 166]
LMR	Humidity	TiO_2 NPs/poly(sodium 4-styrenesulfonate)	LbL	1.43 nm/RH% LMR 1 0.97 nm/RH% LMR 2	[167]
LMR	Humidity	Poly(allylamine hydrochloride)/poly(acrylic acid) + Ag NPs	LbL	0.455 nm/RH%	[168]
LMR	VOCs	Poly(allylamine hydrochloride)/Au-Ag nanocompound + sodium dodecyl sulfate	LbL	0.131 nm/ppm for methanol	[169]

based sensor with Au nanorods coating and SPR based sensor with a thin Au layer, giving the second one higher sensitivity.

7.3. LMR Based Sensors with NP-Embedded Coatings. LMR theory is very recent, and its development in sensing has been reported since 2009 by some authors [156, 178, 179]. Thus, the use of NPs in these sensors is being a hot-point at this moment.

In these few years, LMR based sensors with embedded NPs have been published to measure parameters such as the surrounding RI [165], relative humidity [167], or volatile organic compounds (VOCs) [169] using the LbL technique.

Rivero et al. have recently developed the first sensor where both LSPR and LMR phenomena appear [157], thanks to a self-assembled polymeric coating with Ag NPs. In this work, the appearance and evolution of the LSPR caused by the Ag NPs and LMRs caused by the overall coating, during the LbL deposition process, were observed (shown in Figure 12). As a result, the created coating and its swelling properties produced important changes in the mode resonances, shifting their respective LMR peaks according to the humidity changes (Figure 13). Their results had a sensitivity of 1 nm per RH% from the first LMR. They also show another sensor with 0.943 nm per RH% for the second LMR.

The same research group also developed another refractometer based on both types of resonances, here using Au NP-embedded coatings [164]. Last works in LMR based sensors indicate that this sensing mechanism and its potential use have a promising future in the next years.

Finally, a summary with different approaches of fiber-optic sensors based on LSPR and LMR is shown in Table 2.

8. Conclusions

In this review, a classification of optical fiber sensors based on nanoparticle-embedded coatings is proposed; this list

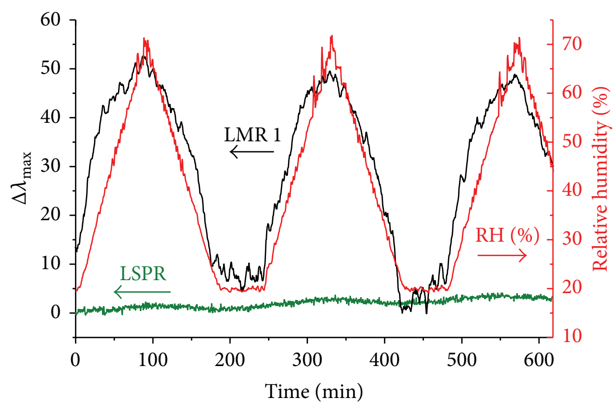

Figure 13: Dynamic response of the sensor. The wavelength shifts of both LSPR and LMR 1 are monitored simultaneously to RH cycles from 20 to 70% RH at 25°C. Reprinted from [157], Copyright (2012) with permission from Elsevier.

of sensors has been ordered according to their sensing principles, which are briefly described in separated sections. Absorbance, interferometry, fluorescence, gratings, and resonances phenomena were briefly reported. The introduction of new specialty fibers combined to these coatings has plenty of potential applications. Moreover, LSPR and LMR technologies in fiber sensing are experiencing a great degree of development these days. All these advances are likely to drive future trends in the research and development of optical fiber sensors.

Conflict of Interests

The authors declare that there is no conflict of interests regarding the publication of this paper.

Acknowledgments

This work was supported in part by the Spanish Ministry of Economy and Competitiveness CICYT-FEDER TEC2013-43679-R Research Grant and a UPNA predoctoral research grant.

References

[1] B. Lee, "Review of the present status of optical fiber sensors," *Optical Fiber Technology*, vol. 9, no. 2, pp. 57–79, 2003.

[2] B. Culshaw, "Optical fiber sensor technologies: opportunities and—perhaps—pitfalls," *Journal of Lightwave Technology*, vol. 22, no. 1, pp. 39–50, 2004.

[3] A. Abdelghani, J. M. Chovelon, N. Jaffrezic-Renault et al., "Optical fibre sensor coated with porous silica layers for gas and chemical vapour detection," *Sensors and Actuators B: Chemical*, vol. 44, no. 1–3, pp. 495–498, 1997.

[4] V. P. Minkovich, D. Monzón-Hernández, J. Villatoro, and G. Badenes, "Microstructured optical fiber coated with thin films for gas and chemical sensing," *Optics Express*, vol. 14, no. 18, pp. 8413–8418, 2006.

[5] J. Lin, "Recent development and applications of optical and fiber-optic pH sensors," *TrAC Trends in Analytical Chemistry*, vol. 19, no. 9, pp. 541–552, 2000.

[6] F. J. Arregui, I. R. Matías, K. L. Cooper, and R. O. Claus, "Simultaneous measurement of humidity and temperature by combining a reflective intensity-based optical fiber sensor and a fiber bragg grating," *IEEE Sensors Journal*, vol. 2, no. 5, pp. 482–487, 2002.

[7] C. Bariáin, I. R. Matías, F. J. Arregui, and M. López-Amo, "Optical fiber humidity sensor based on a tapered fiber coated with agarose gel," *Sensors and Actuators B: Chemical*, vol. 69, no. 1, pp. 127–131, 2000.

[8] S. K. Khijwania, K. L. Srinivasan, and J. P. Singh, "An evanescent-wave optical fiber relative humidity sensor with enhanced sensitivity," *Sensors and Actuators B: Chemical*, vol. 104, no. 2, pp. 217–222, 2005.

[9] S. C. Warren-Smith, S. Heng, H. Ebendorff-Heidepriem, A. D. Abell, and T. M. Monro, "Fluorescence-based aluminum ion sensing using a surface-functionalized microstructured optical fiber," *Langmuir*, vol. 27, no. 9, pp. 5680–5685, 2011.

[10] M. El-Sherif, L. Bansal, and J. Yuan, "Fiber optic sensors for detection of toxic and biological threats," *Sensors*, vol. 7, no. 12, pp. 3100–3118, 2007.

[11] O. S. Wolfbeis, "Fiber-optic chemical sensors and biosensors," *Analytical Chemistry*, vol. 76, no. 12, pp. 3269–3284, 2004.

[12] S. Lepinay, A. Staff, A. Ianoul, and J. Albert, "Improved detection limits of protein optical fiber biosensors coated with gold nanoparticles," *Biosensors and Bioelectronics*, vol. 52, pp. 337–344, 2014.

[13] D. Viegas, J. Goicoechea, J. L. Santos et al., "Sensitivity improvement of a humidity sensor based on silica nanospheres on a long-period fiber grating," *Sensors*, vol. 9, no. 1, pp. 519–527, 2009.

[14] R. Aneesh and S. K. Khijwania, "Zinc oxide nanoparticle based optical fiber humidity sensor having linear response throughout a large dynamic range," *Applied Optics*, vol. 50, no. 27, pp. 5310–5314, 2011.

[15] P. J. Rivero, A. Urrutia, J. Goicoechea, F. J. Arregui, and I. R. Matías, "Humidity sensor based on silver nanoparticles embedded in a polymeric coating," *International Journal on Smart Sensing and Intelligent Systems*, vol. 5, no. 1, pp. 71–83, 2012.

[16] R. N. Mariammal, K. Ramachandran, B. Renganathan, and D. Sastikumar, "On the enhancement of ethanol sensing by CuO modified SnO_2 nanoparticles using fiber-optic sensor," *Sensors and Actuators, B: Chemical*, vol. 169, pp. 199–207, 2012.

[17] L. R. Shobin, D. Sastikumar, and S. Manivannan, "Glycerol mediated synthesis of silver nanowires for room temperature ammonia vapor sensing," *Sensors and Actuators A: Physical*, vol. 214, pp. 74–80, 2014.

[18] B. Renganathan, D. Sastikumar, S. G. Raj, and A. R. Ganesan, "Fiber optic gas sensors with vanadium oxide and tungsten oxide nanoparticle coated claddings," *Optics Communications*, vol. 315, pp. 74–78, 2014.

[19] B. Renganathan, D. Sastikumar, G. Gobi, N. R. Yogamalar, and A. C. Bose, "Gas sensing properties of a clad modified fiber optic sensor with Ce, Li and Al doped nanocrystalline zinc oxides," *Sensors and Actuators B: Chemical*, vol. 156, no. 1, pp. 263–270, 2011.

[20] S. Kodaira, S. Korposh, S.-W. Lee, W. J. Batty, S. W. James, and R. P. Tatam, "Fabrication of highly efficient fibre-optic gas sensors using SiO_2/polymer nanoporous thin films," in *Proceedings of the 3rd International Conference on Sensing Technology (ICST '08)*, pp. 481–485, December 2008.

[21] S. K. Khijwania and B. D. Gupta, "Maximum achievable sensitivity of the fiber optic evanescent field absorption sensor

based on the U-shaped probe," *Optics Communications*, vol. 175, no. 1, pp. 135–137, 2000.

[22] D. Littlejohn, D. Lucas, and L. Han, "Bent silica fiber evanescent absorption sensors for near-infrared spectroscopy," *Applied Spectroscopy*, vol. 53, no. 7, pp. 845–849, 1999.

[23] R. Jindal, S. Tao, J. P. Singh, and P. S. Gaikwad, "High dynamic range fiber optic relative humidity sensor," *Optical Engineering*, vol. 41, no. 5, pp. 1093–1096, 2002.

[24] Z. Zhao and Y. Duan, "A low cost fiber-optic humidity sensor based on silica sol-gel film," *Sensors and Actuators B: Chemical*, vol. 160, no. 1, pp. 1340–1345, 2011.

[25] F. Surre, B. Lyons, T. Sun et al., "U-bend fibre optic pH sensors using layer-by-layer electrostatic self-assembly technique," *Journal of Physics: Conference Series*, vol. 178, Article ID 012046, 2009.

[26] H. Guo and S. Tao, "Silver nanoparticles doped silica nanocomposites coated on an optical fiber for ammonia sensing," *Sensors and Actuators B: Chemical*, vol. 123, no. 1, pp. 578–582, 2007.

[27] A. Vijayan, M. Fuke, R. Hawaldar, M. Kulkarni, D. Amalnerkar, and R. C. Aiyer, "Optical fibre based humidity sensor using Co-polyaniline clad," *Sensors and Actuators B: Chemical*, vol. 129, no. 1, pp. 106–112, 2008.

[28] S. K. Shukla, G. K. Parashar, A. P. Mishra et al., "Nano-like magnesium oxide films and its significance in optical fiber humidity sensor," *Sensors and Actuators B: Chemical*, vol. 98, no. 1, pp. 5–11, 2004.

[29] C.-H. Chen, T.-C. Tsao, W.-Y. Li et al., "Novel U-shape gold nanoparticles-modified optical fiber for localized plasmon resonance chemical sensing," *Microsystem Technologies*, vol. 16, no. 7, pp. 1207–1214, 2010.

[30] R. Bharadwaj and S. Mukherji, "Gold nanoparticle coated U-bend fibre optic probe for localized surface plasmon resonance based detection of explosive vapours," *Sensors and Actuators B: Chemical*, vol. 192, pp. 804–811, 2014.

[31] M. Ahmad and L. L. Hench, "Effect of taper geometries and launch angle on evanescent wave penetration depth in optical fibers," *Biosensors and Bioelectronics*, vol. 20, no. 7, pp. 1312–1319, 2005.

[32] S. Guo and S. Albin, "Transmission property and evanescent wave absorption of cladded multimode fiber tapers," *Optics Express*, vol. 11, no. 3, pp. 215–223, 2003.

[33] A. G. Mignani, R. Falciai, and L. Ciaccheri, "Evanescent wave absorption spectroscopy by means of bi-tapered multimode optical fibers," *Applied Spectroscopy*, vol. 52, no. 4, pp. 546–551, 1998.

[34] D. Rithesh Raj, S. Prasanth, T. V. Vineeshkumar, and C. Sudarsanakumar, "Ammonia sensing properties of tapered plastic optical fiber coated with silver nanoparticles/PVP/PVA hybrid," *Optics Communications*, vol. 340, pp. 86–92, 2015.

[35] A. Aziz, H. N. Lim, S. H. Girei et al., "Silver/graphene nanocomposite-modified optical fiber sensor platform for ethanol detection in water medium," *Sensors and Actuators B: Chemical*, vol. 206, pp. 119–125, 2015.

[36] M. I. Zibaii, H. Latifi, Z. Saeedian, and Z. Chenari, "Nonadiabatic tapered optical fiber sensor for measurement of antimicrobial activity of silver nanoparticles against *Escherichia coli*," *Journal of Photochemistry and Photobiology B: Biology*, vol. 135, pp. 55–64, 2014.

[37] D. Monzón-Hernández, D. Luna-Moreno, D. M. Escobar, and J. Villatoro, "Optical microfibers decorated with PdAu nanoparticles for fast hydrogen sensing," *Sensors and Actuators, B: Chemical*, vol. 151, no. 1, pp. 219–222, 2010.

[38] X. Yang, Y. Liu, F. Tian et al., "Optical fiber modulator derivates from hollow optical fiber with suspended core," *Optics Letters*, vol. 37, no. 11, pp. 2115–2117, 2012.

[39] H. Lu, Z. Tian, H. Yu et al., "Optical fiber with nanostructured cladding of TiO_2 nanoparticles self-assembled onto a side polished fiber and its temperature sensing," *Optics Express*, vol. 22, no. 26, pp. 32502–32508, 2014.

[40] N. J. Florous, K. Saitoh, and M. Koshiba, "Numerical modeling of cryogenic temperature sensors based on plasmonic oscillations in metallic nanoparticles embedded into photonic crystal fibers," *IEEE Photonics Technology Letters*, vol. 19, no. 5, pp. 324–326, 2007.

[41] Y. Miao, B. Liu, K. Zhang, Y. Liu, and H. Zhang, "Temperature tunability of photonic crystal fiber filled with Fe_3O_4 nanoparticle fluid," *Applied Physics Letters*, vol. 98, no. 2, Article ID 021103, 2011.

[42] J. Canning, L. Moura, L. Lindoy et al., "Fabricating nanoporous silica structure on D-fibres through room temperature self-assembly," *Materials*, vol. 7, no. 3, pp. 2356–2369, 2014.

[43] B. H. Lee, Y. H. Kim, K. S. Park et al., "Interferometric fiber optic sensors," *Sensors*, vol. 12, no. 3, pp. 2467–2486, 2012.

[44] A. Wang, H. Xiao, J. Wang, Z. Wang, W. Zhao, and R. G. May, "Self-calibrated interferometric-intensity-based optical fiber sensors," *Journal of Lightwave Technology*, vol. 19, no. 10, pp. 1495–1501, 2001.

[45] X. Chen, F. Shen, Z. Wang, Z. Huang, and A. Wang, "Micro-air-gap based intrinsic Fabry-Perot interferometric fiber-optic sensor," *Applied Optics*, vol. 45, no. 30, pp. 7760–7766, 2006.

[46] F. J. Arregui, Y. Liu, I. R. Matias, and R. O. Claus, "Optical fiber humidity sensor using a nano Fabry-Perot cavity formed by the ionic self-assembly method," *Sensors and Actuators, B: Chemical*, vol. 59, no. 1, pp. 54–59, 1999.

[47] M. Jiang, Q.-S. Li, J.-N. Wang et al., "Optical response of fiber-optic Fabry-Perot refractive-index tip sensor coated with polyelectrolyte multilayer ultra-thin films," *Journal of Lightwave Technology*, vol. 31, no. 14, pp. 2321–2326, 2013.

[48] J. M. Corres, I. R. Matias, M. Hernaez, J. Bravo, and F. J. Arregui, "Optical fiber humidity sensors using nanostructured coatings of SiO_2 nanoparticles," *IEEE Sensors Journal*, vol. 8, no. 3, pp. 281–285, 2008.

[49] S. Dass, R. K. Gangwar, S. M. Nalawade, and T. M. Bhave, "A novel optical fiber humidity sensor coated with superhydrophilic silica nanoparticles," *AIP Conference Proceedings*, vol. 1391, no. 1, pp. 428–430, 2011.

[50] Y.-T. Tseng, Y.-J. Chuang, Y.-C. Wu, C.-S. Yang, M.-C. Wang, and F.-G. Tseng, "A gold-nanoparticle-enhanced immune sensor based on fiber optic interferometry," *Nanotechnology*, vol. 19, no. 34, Article ID 345501, 2008.

[51] M. Jiang, Q.-S. Li, J.-N. Wang et al., "TiO_2 nanoparticle thin film-coated optical fiber Fabry-Perot sensor," *Optics Express*, vol. 21, no. 3, pp. 3083–3090, 2013.

[52] M. Consales, A. Crescitelli, M. Penza et al., "SWCNT nanocomposite optical sensors for VOC and gas trace detection," *Sensors and Actuators B: Chemical*, vol. 138, no. 1, pp. 351–361, 2009.

[53] M. Yin, B. Gu, Q. Zhao et al., "Highly sensitive and fast responsive fiber-optic modal interferometric pH sensor based on polyelectrolyte complex and polyelectrolyte self-assembled nanocoating," *Analytical and Bioanalytical Chemistry*, vol. 399, no. 10, pp. 3623–3631, 2011.

[54] N. Liu, L. Li, G. Cao, and R. Lee, "Silver-embedded zeolite thin film-based fiber optic sensor for *in situ*, real-time monitoring Hg^{2+} ions in aqueous media with high sensitivity and selectivity," *Journal of Materials Chemistry*, vol. 20, no. 41, pp. 9029–9031, 2010.

[55] O. Duhem, J. F. Henninot, and M. Douay, "Study of in fiber Mach-Zehnder interferometer based on two spaced 3-dB long period gratings surrounded by a refractive index higher than that of silica," *Optics Communications*, vol. 180, no. 4, pp. 255–262, 2000.

[56] J. Yang, L. Jiang, S. Wang et al., "High sensitivity of taper-based Mach-Zehnder interferometer embedded in a thinned optical fiber for refractive index sensing," *Applied Optics*, vol. 50, no. 28, pp. 5503–5507, 2011.

[57] S. W. James, S. Korposh, S.-W. Lee, and R. P. Tatam, "A long period grating-based chemical sensor insensitive to the influence of interfering parameters," *Optics Express*, vol. 22, no. 7, pp. 8012–8023, 2014.

[58] B. Li, L. Jiang, S. Wang, L. Zhou, H. Xiao, and T. Hai-Lung, "Ultra-abrupt tapered fiber mach-zehnder interferometer sensors," *Sensors*, vol. 11, no. 6, pp. 5729–5739, 2011.

[59] A. B. Socorro, I. Del Villar, J. M. Corres, F. J. Arregui, and I. R. Matias, "Sensitivity enhancement in a multimode interference-based SMS fibre structure coated with a thin-film: theoretical and experimental study," *Sensors and Actuators, B: Chemical*, vol. 190, pp. 363–369, 2014.

[60] C. Carrasquilla, Y. Xiao, C. Q. Xu, Y. Li, and J. D. Brennan, "Enhancing sensitivity and selectivity of long-period grating sensors using structure-switching aptamers bound to gold-doped macroporous silica coatings," *Analytical Chemistry*, vol. 83, no. 20, pp. 7984–7991, 2011.

[61] H. Y. Fu, H. Y. Tam, L.-Y. Shao et al., "Pressure sensor realized with polarization-maintaining photonic crystal fiber-based Sagnac interferometer," *Applied Optics*, vol. 47, no. 15, pp. 2835–2839, 2008.

[62] L. H. Chen, C. C. Chan, T. Li et al., "Chitosan-coated polarization maintaining fiber-based sagnac interferometer for relative humidity measurement," *IEEE Journal on Selected Topics in Quantum Electronics*, vol. 18, no. 5, pp. 1597–1604, 2012.

[63] J. Wang, H. Liang, X. Dong, and Y. Jin, "A temperature-insensitive relative humidity sensor by using polarization maintaining fiber-based sagnac interferometer," *Microwave and Optical Technology Letters*, vol. 55, no. 10, pp. 2305–2307, 2013.

[64] C. Wu, B.-O. Guan, C. Lu, and H.-Y. Tam, "Salinity sensor based on polyimide-coated photonic crystal fiber," *Optics Express*, vol. 19, no. 21, pp. 20003–20008, 2011.

[65] O. S. Wolfbeis, *Fiber Optic Chemical Sensors and Biosensors*, vol. 1, CRC Press, 1991.

[66] B. D. MacCraith, C. M. McDonagh, G. O'Keeffe et al., "Fibre optic oxygen sensor based on fluorescence quenching of evanescent-wave excited ruthenium complexes in sol-gel derived porous coatings," *Analyst*, vol. 4, no. 118, pp. 385–388, 1993.

[67] D. J. Monk and D. R. Walt, "Optical fiber-based biosensors," *Analytical and Bioanalytical Chemistry*, vol. 379, no. 7-8, pp. 931–945, 2004.

[68] K. L. Brogan and D. R. Walt, "Optical fiber-based sensors: application to chemical biology," *Current Opinion in Chemical Biology*, vol. 9, no. 5, pp. 494–500, 2005.

[69] A. Leung, P. M. Shankar, and R. Mutharasan, "A review of fiber-optic biosensors," *Sensors and Actuators B: Chemical*, vol. 125, no. 2, pp. 688–703, 2007.

[70] T. Yamauchi, H. Iwai, and Y. Yamashita, "Label-free imaging of the dynamics of cell-to-cell string-like structure bridging in the free-space by low-coherent quantitative phase microscopy," in *Optical Coherence Tomography and Coherence Domain Optical Methods in Biomedicine XVII*, vol. 8571 of *Proceedings of SPIE*, March 2013.

[71] H. Deng, Y. Bai, J. Xiao, and Q. Wu, "Precision estimate of fluorescence quenching based fiber optical oxygen sensor," *Optical Technique*, vol. 41, pp. 124–127, 131, 2015.

[72] R. W. Sabnis, *Handbook of Fluorescent Dyes and Probes*, John Wiley & Sons, Hoboken, NJ, USA, 2015.

[73] J. A. Kiernan, "Classification and naming of dyes, stains and fluorochromes," *Biotechnic and Histochemistry*, vol. 76, no. 5-6, pp. 261–277, 2001.

[74] J. Goicoechea, F. J. Arregui, and I. R. Matias, "Quantum dots for sensing," in *Sensors Based on Nanostructured Materials*, F. J. Arregui, Ed., pp. 131–181, Springer, New York, NY, USA, 2008.

[75] J. M. Costa-Fernandez, "Optical sensors based on luminescent quantum dots," *Analytical and Bioanalytical Chemistry*, vol. 384, no. 1, pp. 37–40, 2006.

[76] M. Dahan, S. Lévi, C. Luccardini, P. Rostaing, B. Riveau, and A. Triller, "Diffusion dynamics of glycine receptors revealed by single-quantum dot tracking," *Science*, vol. 302, no. 5644, pp. 442–445, 2003.

[77] L. Zhu, S. Ang, and W.-T. Liu, "Quantum dots as a novel immunofluorescent detection system for *Cryptosporidium parvum* and giardia lamblia," *Applied and Environmental Microbiology*, vol. 70, no. 1, pp. 597–598, 2004.

[78] X. Michalet, F. F. Pinaud, L. A. Bentolila et al., "Quantum dots for live cells, in vivo imaging, and diagnostics," *Science*, vol. 307, no. 5709, pp. 538–544, 2005.

[79] R. Bakalova, Z. Zhelev, H. Ohba, and Y. Baba, "Quantum dot-based western blot technology for ultrasensitive detection of tracer proteins," *Journal of the American Chemical Society*, vol. 127, no. 26, pp. 9328–9329, 2005.

[80] S. C. Makrides, C. Gasbarro, and J. M. Bello, "Bioconjugation of quantum dot luminescent probes for Western blot analysis," *BioTechniques*, vol. 39, no. 4, pp. 501–505, 2005.

[81] A. R. Clapp, I. L. Medintz, J. M. Mauro, B. R. Fisher, M. G. Bawendi, and H. Mattoussi, "Fluorescence resonance energy transfer between quantum dot donors and dye-labeled protein acceptors," *Journal of the American Chemical Society*, vol. 126, no. 1, pp. 301–310, 2004.

[82] A. M. Dennis, W. J. Rhee, D. Sotto, S. N. Dublin, and G. Bao, "Quantum dot-fluorescent protein fret probes for sensing intracellular pH," *ACS Nano*, vol. 6, no. 4, pp. 2917–2924, 2012.

[83] G. de Bastida, F. J. Arregui, J. Goicoechea, and I. R. Matias, "Quantum dots-based optical fiber temperature sensors fabricated by layer-by-layer," *IEEE Sensors Journal*, vol. 6, no. 6, pp. 1378–1379, 2006.

[84] B. Larrió.n, M. Hernáez, F. J. Arregui, J. Goicoechea, J. Bravo, and I. R. Matías, "Photonic crystal fiber temperature sensor based on quantum dot nanocoatings," *Journal of Sensors*, vol. 2009, Article ID 932471, 6 pages, 2009.

[85] M. E. Stewart, C. R. Anderton, L. B. Thompson et al., "Nanostructured plasmonic sensors," *Chemical Reviews*, vol. 108, no. 2, pp. 494–521, 2008.

[86] X. Li, L. Jiang, Q. Zhan, J. Qian, and S. He, "Localized surface plasmon resonance (LSPR) of polyelectrolyte-functionalized gold-nanoparticles for bio-sensing," *Colloids and Surfaces A: Physicochemical and Engineering Aspects*, vol. 332, no. 2-3, pp. 172–179, 2009.

[87] Y. Wang, B. Liu, A. Mikhailovsky, and G. C. Bazan, "Conjugated polyelectrolyte-metal nanoparticle platforms for optically amplified dna detection," *Advanced Materials*, vol. 22, no. 5, pp. 656–659, 2010.

[88] J. Geng, J. Liang, Y. Wang, G. G. Gurzadyan, and B. Liu, "Metal-enhanced fluorescence of conjugated polyelectrolytes with self-assembled silver nanoparticle platforms," *Journal of Physical Chemistry B*, vol. 115, no. 13, pp. 3281–3288, 2011.

[89] N. Ma, F. Tang, X. Wang, F. He, and L. Li, "Tunable metal-enhanced fluorescence by stimuli-responsive polyelectrolyte interlayer films," *Macromolecular Rapid Communications*, vol. 32, no. 7, pp. 587–592, 2011.

[90] J. Zhang, N. Ma, F. Tang, Q. Cui, F. He, and L. Li, "pH- and glucose-responsive core-shell hybrid nanoparticles with controllable metal-enhanced fluorescence effects," *ACS Applied Materials and Interfaces*, vol. 4, no. 3, pp. 1747–1751, 2012.

[91] A. M. Gabudean, M. Focsan, and S. Astilean, "Gold nanorods performing as dual-modal nanoprobes via metal-enhanced fluorescence (MEF) and surface-enhanced Raman scattering (SERS)," *Journal of Physical Chemistry C*, vol. 116, no. 22, pp. 12240–12249, 2012.

[92] C. L. Haynes and R. P. Van Duyne, "Plasmon-sampled surface-enhanced Raman excitation spectroscopy," *Journal of Physical Chemistry B*, vol. 107, no. 30, pp. 7426–7433, 2003.

[93] L. A. Dick, A. D. McFarland, C. L. Haynes, and R. P. Van Duyne, "Metal film over nanosphere (MFON) electrodes for surface-enhanced Raman spectroscopy (SERS): improvements in surface nanostructure stability and suppression of irreversible loss," *Journal of Physical Chemistry B*, vol. 106, no. 4, pp. 853–860, 2002.

[94] J. Cao, D. Zhao, X. Lei, Y. Liu, and Q. Mao, "One-pot hydrothermal synthesis of silver nanoplates on optical fiber tip for surface-enhanced Raman scattering," *Applied Physics Letters*, vol. 104, no. 20, Article ID 201906, 2014.

[95] L. X. Quang, C. Lim, G. H. Seong, J. Choo, K. J. Do, and S.-K. Yoo, "A portable surface-enhanced Raman scattering sensor integrated with a lab-on-a-chip for field analysis," *Lab on a Chip*, vol. 8, no. 12, pp. 2214–2219, 2008.

[96] A. Walter, A. März, W. Schumacher, P. Rösch, and J. Popp, "Towards a fast, high specific and reliable discrimination of bacteria on strain level by means of SERS in a microfluidic device," *Lab on a Chip—Miniaturisation for Chemistry and Biology*, vol. 11, no. 6, pp. 1013–1021, 2011.

[97] Z. Chen, Z. Dai, N. Chen et al., "Gold nanoparticles-modified tapered fiber nanoprobe for remote SERS detection," *IEEE Photonics Technology Letters*, vol. 26, no. 8, pp. 777–780, 2014.

[98] D. Jin, Y. Bai, H. Chen et al., "SERS detection of expired tetracycline hydrochloride with an optical fiber nano-probe," *Analytical Methods*, vol. 7, no. 4, pp. 1307–1312, 2015.

[99] C. Liu, S. Wang, G. Chen et al., "A surface-enhanced Raman scattering (SERS)-active optical fiber sensor based on a three-dimensional sensing layer," *Sensing and Bio-Sensing Research*, vol. 1, pp. 8–14, 2014.

[100] C. Liu, S. Wang, C. Fu, H. Li, S. Xu, and W. Xu, "Preparation of surface-enhanced Raman scattering(SERS)-active optical fiber sensor by laser-induced Ag deposition and its application in bioidentification of biotin/avidin," *Chemical Research in Chinese Universities*, vol. 31, no. 1, pp. 25–30, 2015.

[101] A. Dragomir, D. N. Nikogosyan, K. A. Zagorulko, P. G. Kryukov, and E. M. Dianov, "Inscription of fiber Bragg gratings by ultraviolet femtosecond radiation," *Optics Letters*, vol. 28, no. 22, pp. 2171–2173, 2003.

[102] Y.-J. Rao, Y.-P. Wang, Z.-L. Ran, and T. Zhu, "Novel fiber-optic sensors based on long-period fiber gratings written by high-frequency CO_2 laser pulses," *Journal of Lightwave Technology*, vol. 21, no. 5, pp. 1320–1327, 2003.

[103] Y. Kondo, K. Nouchi, T. Mitsuyu, M. Watanabe, P. G. Kazansky, and K. Hirao, "Fabrication of long-period fiber gratings by focused irradiation of infrared femtosecond laser pulses," *Optics Letters*, vol. 24, no. 10, pp. 646–648, 1999.

[104] A. Malki, G. Humbert, Y. Ouerdane, A. Boukhenter, and A. Boudrioua, "Investigation of the writing mechanism of electric-arc-induced long-period fiber gratings," *Applied Optics*, vol. 42, no. 19, pp. 3776–3779, 2003.

[105] K. O. Hill and G. Meltz, "Fiber Bragg grating technology fundamentals and overview," *Journal of Lightwave Technology*, vol. 15, no. 8, pp. 1263–1276, 1997.

[106] A. D. Kersey, M. A. Davis, H. J. Patrick et al., "Fiber grating sensors," *Journal of Lightwave Technology*, vol. 15, no. 8, pp. 1442–1462, 1997.

[107] T. Erdogan, "Fiber grating spectra," *Journal of Lightwave Technology*, vol. 15, no. 8, pp. 1277–1294, 1997.

[108] A. M. Vengsarkar, P. J. Lemaire, J. B. Judkins, V. Bhatia, T. Erdogan, and J. E. Sipe, "Long-period fiber gratings as band-rejection filters," *Journal of Lightwave Technology*, vol. 14, no. 1, pp. 58–64, 1996.

[109] S. W. James and R. P. Tatam, "Optical fibre long-period grating sensors: characteristics and application," *Measurement Science and Technology*, vol. 14, no. 5, pp. R49–R61, 2003.

[110] V. Bhatia, "Applications of long-period gratings to single and multi-parameter sensing," *Optics Express*, vol. 4, no. 11, pp. 457–466, 1999.

[111] X.-K. Zeng and Y.-J. Rao, "Simultaneous static strain, temperature and vibration measurement using an integrated FBG/EFPI sensor," *Chinese Physics Letters*, vol. 18, no. 12, pp. 1617–1619, 2001.

[112] Z. C. Zhuo and B. S. Ham, "A temperature-insensitive strain sensor using a fiber Bragg grating," *Optical Fiber Technology*, vol. 15, no. 5-6, pp. 442–444, 2009.

[113] J. Jung, H. Nam, B. Lee, J. O. Byun, and N. S. Kim, "Fiber Bragg grating temperature sensor with controllable sensitivity," *Applied Optics*, vol. 38, no. 13, pp. 2752–2754, 1999.

[114] H. Ahmad, W. Y. Chong, K. Thambiratnam et al., "High sensitivity fiber Bragg grating pressure sensor using thin metal diaphragm," *IEEE Sensors Journal*, vol. 9, no. 12, pp. 1654–1659, 2009.

[115] X. Dong, H. Zhang, B. Liu, and Y. Miao, "Tilted fiber bragg gratings: principle and sensing applications," *Photonic Sensors*, vol. 1, no. 1, pp. 6–30, 2011.

[116] S. C. Kang, S. Y. Kim, S. B. Lee, S. W. Kwon, S. S. Choi, and B. Lee, "Temperature-independent strain sensor system using a tilted fiber bragg grating demodulator," *IEEE Photonics Technology Letters*, vol. 10, no. 10, pp. 1461–1463, 1998.

[117] E. Chehura, S. W. James, and R. P. Tatam, "Temperature and strain discrimination using a single tilted fibre Bragg grating," *Optics Communications*, vol. 275, no. 2, pp. 344–347, 2007.

[118] T. Guo, A. Ivanov, G. Chen, and J. Albert, "Temperature-independent tilted fiber grating vibration sensor based on cladding-core recoupling," *Optics Letters*, vol. 33, no. 9, pp. 1004–1006, 2008.

[119] S. Baek, Y. Jeong, and B. Lee, "Characteristics of short-period blazed fiber Bragg gratings for use as macro-bending sensors," *Applied Optics*, vol. 41, no. 4, pp. 631–636, 2002.

[120] X. Chen, K. Zhou, L. Zhang, and I. Bennion, "In-fiber twist sensor based on a fiber Bragg grating with 81° tilted structure," *IEEE Photonics Technology Letters*, vol. 18, no. 24, pp. 2596–2598, 2006.

[121] C.-L. Zhao, X. Yang, M. S. Demokan, and W. Jin, "Simultaneous temperature and refractive index measurements using a 3° slanted multimode fiber Bragg grating," *Journal of Lightwave Technology*, vol. 24, no. 2, pp. 879–883, 2006.

[122] Y. Miao, B. Liu, H. Zhang et al., "Relative humidity sensor based on tilted fiber Bragg grating with polyvinyl alcohol coating," *IEEE Photonics Technology Letters*, vol. 21, no. 7, pp. 441–443, 2009.

[123] V. Voisin, J. Pilate, P. Damman, P. Mégret, and C. Caucheteur, "Highly sensitive detection of molecular interactions with plasmonic optical fiber grating sensors," *Biosensors and Bioelectronics*, vol. 51, pp. 249–254, 2014.

[124] J.-M. Renoirt, C. Zhang, M. Debliquy, M.-G. Olivier, P. Mégret, and C. Caucheteur, "High-refractive-index transparent coatings enhance the optical fiber cladding modes refractometric sensitivity," *Optics Express*, vol. 21, no. 23, pp. 29073–29082, 2013.

[125] D. Paladino, A. Cusano, P. Pilla, S. Campopiano, C. Caucheteur, and P. Mégret, "Spectral behavior in nano-coated tilted fiber Bragg gratings: effect of thickness and external refractive index," *IEEE Photonics Technology Letters*, vol. 19, no. 24, pp. 2051–2053, 2007.

[126] A. Bialiayeu, A. Bottomley, D. Prezgot, A. Ianoul, and J. Albert, "Plasmon-enhanced refractometry using silver nanowire coatings on tilted fibre Bragg gratings," *Nanotechnology*, vol. 23, no. 44, Article ID 444012, 2012.

[127] A. Cusano, A. Iadicicco, P. Pilla et al., "Mode transition in high refractive index coated long period gratings," *Optics Express*, vol. 14, no. 1, pp. 19–34, 2006.

[128] A. Cusano, A. Iadicicco, P. Pilla et al., "Coated long-period fiber gratings as high-sensitivity optochemical sensors," *Journal of Lightwave Technology*, vol. 24, no. 4, pp. 1776–1786, 2006.

[129] A. Cusano, P. Pilla, L. Contessa et al., "High-sensitivity optical chemosensor based on coated long-period gratings for sub-ppm chemical detection in water," *Applied Physics Letters*, vol. 87, Article ID 234105, pp. 1–3, 2005.

[130] P. Pilla, A. Iadicicco, L. Contessa et al., "Optical chemo-sensor based on long period gratings coated with δ form syndiotactic polystyrene," *IEEE Photonics Technology Letters*, vol. 17, no. 8, pp. 1713–1715, 2005.

[131] G. Decher, "Fuzzy nanoassemblies: toward layered polymeric multicomposites," *Science*, vol. 277, no. 5330, pp. 1232–1237, 1997.

[132] X. Zhang, H. Chen, and H. Zhang, "Layer-by-layer assembly: from conventional to unconventional methods," *Chemical Communications*, pp. 1395–1405, 2007.

[133] P. Sigmund, "Elements of sputtering theory," *Nanofabrication by Ion-Beam Sputtering: Fundamentals and Applications*, pp. 1–40, 2012.

[134] A. Trouillet, E. Marin, and C. Veillas, "Fibre gratings for hydrogen sensing," *Measurement Science and Technology*, vol. 17, no. 5, pp. 1124–1128, 2006.

[135] X. Wei, T. Wei, H. Xiao, and Y. S. Lin, "Nano-structured Pd-long period fiber gratings integrated optical sensor for hydrogen detection," *Sensors and Actuators, B: Chemical*, vol. 134, no. 2, pp. 687–693, 2008.

[136] J. M. Corres, I. Del Villar, I. R. Matias, and F. J. Arregui, "Fiber-optic pH-sensors in long-period fiber gratings using electrostatic self-assembly," *Optics Letters*, vol. 32, no. 1, pp. 29–31, 2007.

[137] J. M. Corres, I. Del Villar, I. R. Matias, and F. J. Arregui, "Two-layer nanocoatings in long-period fiber gratings for improved sensitivity of humidity sensors," *IEEE Transactions on Nanotechnology*, vol. 7, no. 4, pp. 394–400, 2008.

[138] S. M. Topliss, S. W. James, F. Davis, S. P. J. Higson, and R. P. Tatam, "Optical fibre long period grating based selective vapour sensing of volatile organic compounds," *Sensors and Actuators, B: Chemical*, vol. 143, no. 2, pp. 629–634, 2010.

[139] I. Del Villar, I. R. Matias, and F. J. Arregui, "Enhancement of sensitivity in long-period fiber gratings with deposition of low-refractive-index materials," *Optics Letters*, vol. 30, no. 18, pp. 2363–2365, 2005.

[140] I. Del Villar, M. Achaerandio, I. R. Matías, and F. J. Arregui, "Deposition of overlays by electrostatic self-assembly in long-period fiber gratings," *Optics Letters*, vol. 30, no. 7, pp. 720–722, 2005.

[141] X. Shu, L. Zhang, and I. Bennion, "Sensitivity characteristics of long-period fiber gratings," *Journal of Lightwave Technology*, vol. 20, no. 2, pp. 255–266, 2002.

[142] C. S. Cheung, S. M. Topliss, S. W. James, and R. P. Tatam, "Response of fiber-optic long-period gratings operating near the phase-matching turning point to the deposition of nanostructured coatings," *Journal of the Optical Society of America B: Optical Physics*, vol. 25, no. 6, pp. 897–902, 2008.

[143] D. Viegas, J. Goicoechea, J. M. Corres et al., "A fibre optic humidity sensor based on a long-period fibre grating coated with a thin film of SiO_2 nanospheres," *Measurement Science and Technology*, vol. 20, no. 3, Article ID 034002, 2009.

[144] D. Viegas, M. Hernaez, J. Goicoechea et al., "Simultaneous measurement of humidity and temperature based on an SiO_2-nanospheres film deposited on a long-period grating in-line with a fiber Bragg grating," *IEEE Sensors Journal*, vol. 11, no. 1, pp. 162–166, 2011.

[145] J.-L. Tang and J.-N. Wang, "Measurement of chloride-ion concentration with long-period grating technology," *Smart Materials and Structures*, vol. 16, no. 3, pp. 665–672, 2007.

[146] M. Konstantaki, A. Klini, D. Anglos, and S. Pissadakis, "An ethanol vapor detection probe based on a ZnO nanorod coated optical fiber long period grating," *Optics Express*, vol. 20, no. 8, pp. 8472–8484, 2012.

[147] S. Korposh, R. Selyanchyn, W. Yasukochi, S.-W. Lee, S. W. James, and R. P. Tatam, "Optical fibre long period grating with a nanoporous coating formed from silica nanoparticles for ammonia sensing in water," *Materials Chemistry and Physics*, vol. 133, no. 2-3, pp. 784–792, 2012.

[148] S. W. James, S. Korposh, S.-W. Lee, and R. P. Tatam, "A long period grating-based chemical sensor insensitive to the influence of interfering parameters," *Optics Express*, vol. 22, no. 7, pp. 8012–8023, 2014.

[149] R.-Z. Yang, W.-F. Dong, X. Meng et al., "Nanoporous TiO_2/polyion thin-film-coated long-period grating sensors for the direct measurement of low-molecular-weight analytes," *Langmuir*, vol. 28, no. 23, pp. 8814–8821, 2012.

[150] S. Korposh, S.-W. Lee, S. W. James, and R. P. Tatam, "Refractive index sensitivity of fibre-optic long period gratings coated with SiO_2 nanoparticle mesoporous thin films," *Measurement Science and Technology*, vol. 22, no. 7, Article ID 075208, 2011.

[151] L. Marques, F. U. Hernandez, S. Korposh et al., "Sensitive protein detection using an optical fibre long period grating sensor anchored with silica core gold shell nanoparticles," in *23rd International Conference on Optical Fibre Sensors*, vol. 9157 of *Proceedings of SPIE*, Santander, Spain, June 2014.

[152] S. Korposh, T. Wang, S. James, R. Tatam, and S.-W. Lee, "Pronounced aromatic carboxylic acid detection using a layer-by-layer mesoporous coating on optical fibre long period grating," *Sensors and Actuators B: Chemical*, vol. 173, pp. 300–309, 2012.

[153] Y. Huang, Z. Gao, G. Chen, and H. Xiao, "Long period fiber grating sensors coated with nano iron/silica particles for corrosion monitoring," *Smart Materials and Structures*, vol. 22, no. 7, Article ID 075018, 2013.

[154] Y. Huang, F. Tang, X. Liang, G. Chen, H. Xiao, and F. Azarmi, "Steel bar corrosion monitoring with long-period fiber grating sensors coated with nano iron/silica particles and polyurethane," *Structural Health Monitoring*, vol. 14, pp. 178–189, 2015.

[155] J.-L. Tang and J.-N. Wang, "Chemical sensing sensitivity of long-period grating sensor enhanced by colloidal gold nanoparticles," *Sensors*, vol. 8, no. 1, pp. 171–184, 2008.

[156] F. J. Arregui, I. Del Villar, J. M. Corres et al., "Fiber-optic lossy mode resonance sensors," *Procedia Engineering*, vol. 87, pp. 3–8, 2014.

[157] P. J. Rivero, A. Urrutia, J. Goicoechea, and F. J. Arregui, "Optical fiber humidity sensors based on Localized Surface Plasmon Resonance (LSPR) and Lossy-mode resonance (LMR) in overlays loaded with silver nanoparticles," *Sensors and Actuators B: Chemical*, vol. 173, pp. 244–249, 2012.

[158] I.-C. Chen, S.-S. Lin, T.-J. Lin, and J.-K. du, "Detection of hydrofluoric acid by a SiO_2 sol-gel coating fiber-optic probe based on reflection-based localized surface plasmon resonance," *Sensors*, vol. 11, no. 2, pp. 1907–1923, 2011.

[159] P. Bhatia, P. Yadav, and B. D. Gupta, "Surface plasmon resonance based fiber optic hydrogen peroxide sensor using polymer embedded nanoparticles," *Sensors and Actuators, B: Chemical*, vol. 182, pp. 330–335, 2013.

[160] V. V. R. Sai, T. Kundu, and S. Mukherji, "Novel U-bent fiber optic probe for localized surface plasmon resonance based biosensor," *Biosensors and Bioelectronics*, vol. 24, no. 9, pp. 2804–2809, 2009.

[161] R. Dahint, E. Trileva, H. Acunman et al., "Optically responsive nanoparticle layers for the label-free analysis of biospecific interactions in array formats," *Biosensors and Bioelectronics*, vol. 22, no. 12, pp. 3174–3181, 2007.

[162] S. K. Srivastava, V. Arora, S. Sapra, and B. D. Gupta, "Localized surface plasmon resonance-based fiber optic u-shaped biosensor for the detection of blood glucose," *Plasmonics*, vol. 7, no. 2, pp. 261–268, 2012.

[163] A. Candiani, A. Bertucci, S. Giannetti et al., "Label-free DNA biosensor based on a peptide nucleic acid-functionalized microstructured optical fiber-Bragg grating," *Journal of Biomedical Optics*, vol. 18, no. 5, Article ID 057004, 2013.

[164] P. J. Rivero, M. Hernaez, J. Goicoechea, I. R. Matias, and F. J. Arregui, "Optical fiber refractometers based on localized surface plasmon resonance (LSPR) and lossy mode resonance (LMR)," in *23rd International Conference on Optical Fibre Sensors*, vol. 9157 of *Proceedings of SPIE*, International Society for Optical Engineering, Santander, Spain, June 2014.

[165] M. Hernaez, C. R. Zamarreño, I. Del Villar, I. R. Matias, and F. J. Arregui, "Lossy mode resonances supported by TiO_2-coated optical fibers," *Procedia Engineering*, vol. 5, pp. 1099–1102, 2010.

[166] M. Hernáez, I. D. Villar, C. R. Zamarreño, F. J. Arregui, and I. R. Matias, "Optical fiber refractometers based on lossy mode resonances supported by TiO_2 coatings," *Applied Optics*, vol. 49, no. 20, pp. 3980–3985, 2010.

[167] C. R. Zamarreño, M. Hernaez, P. Sanchez, I. Del Villar, I. R. Matias, and F. J. Arregui, "Optical fiber humidity sensor based on lossy mode resonances supported by TiO_2/PSS coatings," *Procedia Engineering*, vol. 25, pp. 1385–1388, 2011.

[168] P. J. Rivero, A. Urrutia, J. Goicoechea, I. R. Matias, and F. J. Arregui, "A Lossy Mode Resonance optical sensor using silver nanoparticles-loaded films for monitoring human breathing," *Sensors and Actuators, B: Chemical*, vol. 187, pp. 40–44, 2013.

[169] C. Elosua, F. J. Arregui, C. R. Zamarreño et al., "Volatile organic compounds optical fiber sensor based on lossy mode resonances," *Sensors and Actuators B: Chemical*, vol. 173, pp. 523–529, 2012.

[170] T. E. Batchman and G. M. McWright, "Mode coupling between dielectric and semiconductor planar waveguides," *IEEE Journal of Quantum Electronics*, vol. 18, no. 4, pp. 782–788, 1982.

[171] M. Marciniak, J. Grzegorzewski, and M. Szustakowski, "Analysis of lossy mode cut-off conditions in planar waveguides with semiconductor guiding layer," *IEE proceedings. Part J, Optoelectronics*, vol. 140, no. 4, pp. 247–252, 1993.

[172] I. Del Villar, C. R. Zamarreño, M. Hernaez, F. J. Arregui, and I. R. Matias, "Generation of lossy mode resonances with absorbing thin-films," *Journal of Lightwave Technology*, vol. 28, no. 23, pp. 3351–3357, 2010.

[173] R. C. Jorgenson and S. S. Yee, "A fiber-optic chemical sensor based on surface plasmon resonance," *Sensors and Actuators: B. Chemical*, vol. 12, no. 3, pp. 213–220, 1993.

[174] X. D. Hoa, A. G. Kirk, and M. Tabrizian, "Towards integrated and sensitive surface plasmon resonance biosensors: a review of recent progress," *Biosensors and Bioelectronics*, vol. 23, no. 2, pp. 151–160, 2007.

[175] B. Sepúlveda, P. C. Angelomé, L. M. Lechuga, and L. M. Liz-Marzán, "LSPR-based nanobiosensors," *Nano Today*, vol. 4, no. 3, pp. 244–251, 2009.

[176] B. D. Gupta and R. K. Verma, "Surface plasmon resonance-based fiber optic sensors: principle, probe designs, and some applications," *Journal of Sensors*, vol. 2009, Article ID 979761, 12 pages, 2009.

[177] J. Cao, E. K. Galbraith, T. Sun, and K. T. V. Grattan, "Cross-comparison of surface plasmon resonance-based optical fiber sensors with different coating structures," *IEEE Sensors Journal*, vol. 12, no. 7, pp. 2355–2361, 2012.

[178] I. Del Villar, C. R. Zamarreño, P. Sanchez et al., "Generation of lossy mode resonances by deposition of high-refractive-index coatings on uncladded multimode optical fibers," *Journal of Optics*, vol. 12, no. 9, Article ID 095503, 2010.

[179] N. Paliwal and J. John, "Theoretical modeling of lossy mode resonance based refractive index sensors with ITO/TiO_2 bilayers," *Applied Optics*, vol. 53, no. 15, pp. 3241–3246, 2014.


Journal of Engineering
The Scientific World Journal
International Journal of Rotating Machinery
Journal of Sensors
International Journal of Distributed Sensor Networks
Advances in Civil Engineering
Hindawi
Submit your manuscripts at
http://www.hindawi.com
Journal of Control Science and Engineering
Journal of Robotics
Journal of Electrical and Computer Engineering
Advances in OptoElectronics
VLSI Design
International Journal of Navigation and Observation
Modelling & Simulation in Engineering
International Journal of Aerospace Engineering
International Journal of Chemical Engineering
International Journal of Antennas and Propagation
Active and Passive Electronic Components
Shock and Vibration
Advances in Acoustics and Vibration